National Défense
Defence nationale

LABORATORY EVALUATION OF THE STANDARD ELEKTRIK LORENZ (SEL) FIBRE-OPTIC RATE GYROSCOPE

by

M.F. Vinnins and L.D. Gallop

DEFENCE RESEARCH ESTABLISHMENT OTTAWA
REPORT NO. 1210

Canada

November 1993
Ottawa

National Défense
Defence nationale

LABORATORY EVALUATION OF THE STANDARD ELEKTRIK LORENZ (SEL) FIBRE-OPTIC RATE GYROSCOPE

by

M.F. Vinnins and L.D. Gallop
Communications and Navigation Section
Electronics Division

DEFENCE RESEARCH ESTABLISHMENT OTTAWA
REPORT NO. 1210

PCN
041LJ

November 1993
Ottawa

ABSTRACT

A fibre-optic rate-sensing gyroscope (FOG) manufactured by Standard Elektrick Lorenz (SEL) was loaned to DREO for evaluation. The SEL FOG, model PM1DE, was designed for a drift rate of 10 to 100 deg/hr and consists of two units; a fibre-optic sensor and a support electronics unit. Laboratory tests were carried out in the DREO Inertial Navigation Laboratory and consisted of bias drift and scale factor over ± 400 deg/sec as well as temperature sensitivity. Performance data obtained by DREO agreed closely with predicted performance although bias drift demonstrated wide deviations under thermal rate-transients. A permanent shift in bias drift and scale factor also occured after extended testing at 50°C. A bias drift of 5.38 deg/hr ± 0.68 deg/hr was achieved at 30°C and scale factor deviation was ≈ 13,000 ppm over a rate range of 400 deg/sec. This instrument would be suitable for a low-performance Attitude and Heading Reference System (AHRS) application.

RÉSUMÉ

Un gyroscope capteur d'allure à fibres optiques (FOG) fabriqué par Standard Elektrick Lorenz (SEL) a été prêté au CRDO pour en faire l'évaluation. Le SEL FOG, modèle PM1DE, a été conçu pour un taux de dérive de 10 à 100 deg/hre et est constitué de deux appareils: un capteur à fibres optiques et un appareil de soutien électronique. Les épreuves conduites au Laboratoire de navigation par inertie portaient sur la dérive de l'erreur systématique et le facteur de proportionnalité de ± 400 deg/sec, ainsi que sur des épreuves de sensibilité thermique avec une plage d'utilisation de 30°C à 60°C. Les données relatives à la performance du gyroscope obtenues par le CRDO correspondaient de près aux prédictions pour la performance, quoique la dérive de l'erreur systématique ait démontré de grands écarts avec les phénomènes transitoires de la température nominale. Un renversement définitif de la dérive de l'erreur systématique et du facteur de proportionnalité s'est également produit après des épreuves prolongées à 50°C. Une dérive de l'erreur de 5.38 deg/hre ± 0.68 deg/hre a été atteinte à 30°C et l'écart du facteur de proportionnalité était de ≈ 13 000 millionièmes par rapport à une variation de taux de 400 deg/sec. Cet instrument serait approprié à des applications à faible performance pour la centrale de cap et de verticale (AHRS).

EXECUTIVE SUMMARY

Several fibre-optic rate gyroscopes, (FOG's) designed and built by Standard Elektrik Lorenz (SEL) AG of Stuttgart, were obtained by Defence Research Establishment Suffield (DRES) for use in an autopilot for a Remotely Piloted Vehicle (RPV). One of the gyroscopes was loaned to DREO for detailed laboratory evaluation. The SEL FOG, model PM1DE, was originally designed for a specific military market; a 10 to 100 deg/hr drift range with input rates up to 1000 deg/sec. Target applications include use in an Attitude and Heading Reference System (AHRS) or integrated into a tightly coupled GPS/INS navigation system.

The FOG unit consists of optics, digital readout electronics and a power supply. The fibre sensing coil is 100 metres long and has a 34 mm radius. The output signal is a 16-bit (parallel) digital signal proportional to rotation rate.

A complete series of laboratory tests were carried out in the DREO Inertial Navigation Laboratory on a Contraves 2-axis motion table. Tests included bias drift (magnitude, stability, repeatability and temperature sensitivity) and scale factor (linearity, stability, repeatability and temperature sensitivity) over a rate range of $\pm$ 400 deg/sec. Turn-on and thermal transient tests were also conducted. A total of 480 hours of test data was accumulated and analyzed.

Gyroscope performance data agreed well with both predicted performance and limited test results as provided by SEL except in scale factor linearity. Bias drift at a nominal operating temperature of 30°C was $\approx$ 5.38 deg/hr $\pm$ 0.68 deg/hr and scale factor deviation was found to be $\approx$ 13,000 ppm over the entire $\pm$ 400 deg/sec rate range; larger than expected.

Both bias and scale factor exhibited substantial temperature sensitivity and, in particular, thermal transients created very large bias shifts if applied quickly.

The SEL FOG performed reliably and, as one of the first commercially -available instruments of its kind, should perform well in low-grade, angular rate sensing applications.

TABLE OF CONTENTS

1.0 INTRODUCTION

This chapter describes the Standard Electrik Lorenz (SEL) Fibre Optic Gyroscope (FOG) and its support electronics and reviews performance specifications as provided by the manufacturer.

The gyroscope, model PM1DE, S/N 88/00021, was manufactured in 1988 and sold to Defence Research Establishment Suffield (DRES). The instrument was loaned to DREO for laboratory evaluation in April 1992. The evaluation was carried out between December 1992 and February 1993. A total of approximately 480 hours of testing was performed.

1.1 The SEL Fibre Optic Gyroscope

The SEL gyroscope is a single axis rate gyro commonly referred to as an Interferometric Fibre Optic Gyroscope (IFOG). It consists of four components:

- semiconductor laser diode light source
- beam splitter
- coil of optical fibre
- photodetector.

These are illustrated in Figure 1.

The principle of operation of an IFOG is similar to that of the Ring Laser Gyroscope (RLG) in that rotation rate is measured by means of ring interferometry [1]. In the IFOG, the light from the laser diode is divided into two beams of almost equal intensity by the beam splitter and one beam is passed clockwise through the fibre coil while the other is passed counter clockwise. The two beams are then superimposed at the photodetector and the interference pattern is monitored.

Rotation about the axis of the fibre coil results in the light travelling in the direction of rotation having a longer propagation time than the light travelling in the opposite direction (the Sagnac effect). This causes a phase shift between the two beams.

The phase shift results in a change in the intensity of the interference signal. The photodetector converts this to an electrical signal which is then digitized into a signal proportional to the rotation rate.

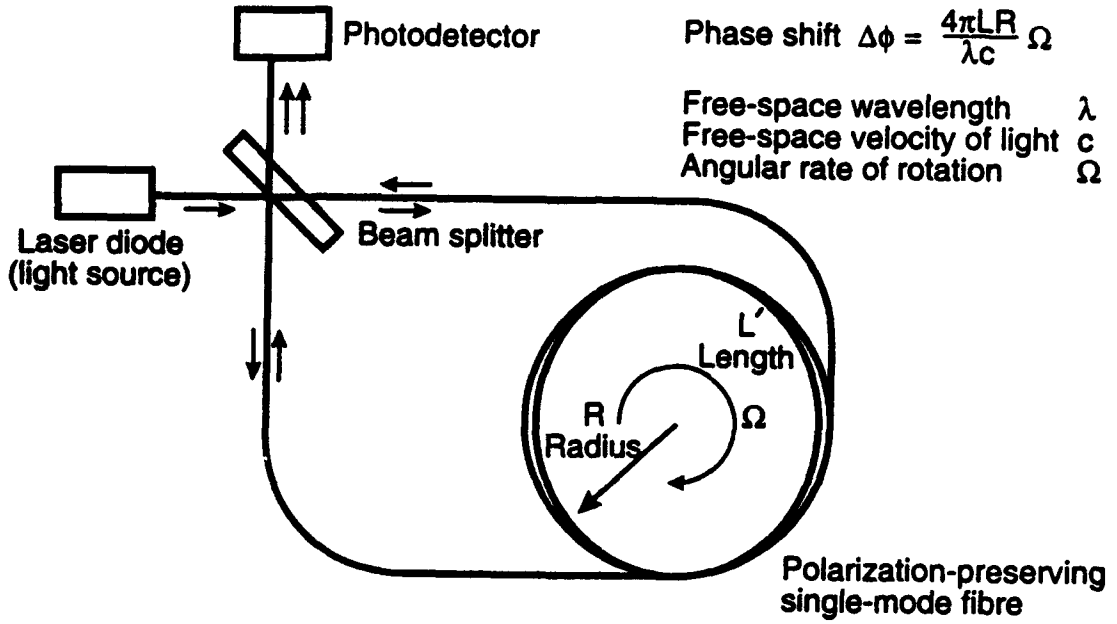

FIGURE 1: Principle of the Fibre Optic Gyroscope

As illustrated in Figure 1, the phase shift, $\Delta\phi$, is proportional to the fibre length L, the coil radius R, and the rotation rate Ω as given by:

$$\Delta\phi = \frac{4\,\pi\,L\,R}{\lambda\,C}\quad \Omega$$

where λ = free space wave length
C = free space velocity
Ω = angular rate of rotation

For the SEL FOG, with a fibre coil length of one hundred metres, an input of one degree per hour will generate a Sagnac phase shift of one microradian.

The SEL FOG contains three basic elements [2]:

a. Optics unit consisting of the fibre coil, light source and photodetector.

b. Digital readout electronics which performs the necessary signal processing and provides a scaled digital rotation rate output.

c. Power supply providing controlled voltage inputs to the readout electronics.

Figures 2 and 3 show functional block diagrams of the electronics and the optics respectively, of the SEL FOG. The electronics consist of a preamplifier and bandpass filter in a miniaturized hybrid circuit. An 8-bit, 4 MHz A/D flash converter provides digitization of the detector output signal, which is then fed to a signal processor for scaling, modelling and scale factor stabilization.

The optics consist of a laser diode light source, contained within the Source Module, whose light passes through the Fibre Coupler into the Integrated Optics Circuit (IOC). The IOC combines the functions of a polarizer, beam splitter and optical phase modulator providing two output beams which are fed to the Fibre Spool. The fibre is a polarization-preserving, single-mode fibre coiled on a metallic carrier with a silicone buffer layer. The carrier is rigidly mounted to the gyro housing, thus providing the reference plane for the gyro input axis.

The Detector Module consists of a photodetector with a hybrid preamplifier.

Details on the signal processing scheme employed by SEL are contained in the literature [2] and will not be further explained here. It is to be noted also that this instrument was designed for a specific rate gyroscope market segment; that being the 10 to 100 deg/hr drift range with input rates to 1000 deg/sec (and higher).

1.2 FOG Performance Specifications

Target specifications for the SEL fibre optic gyroscope, model PM1DE, are contained in Table 1 [3].

A detailed description of the output data format and data recording is contained in the following chapter.

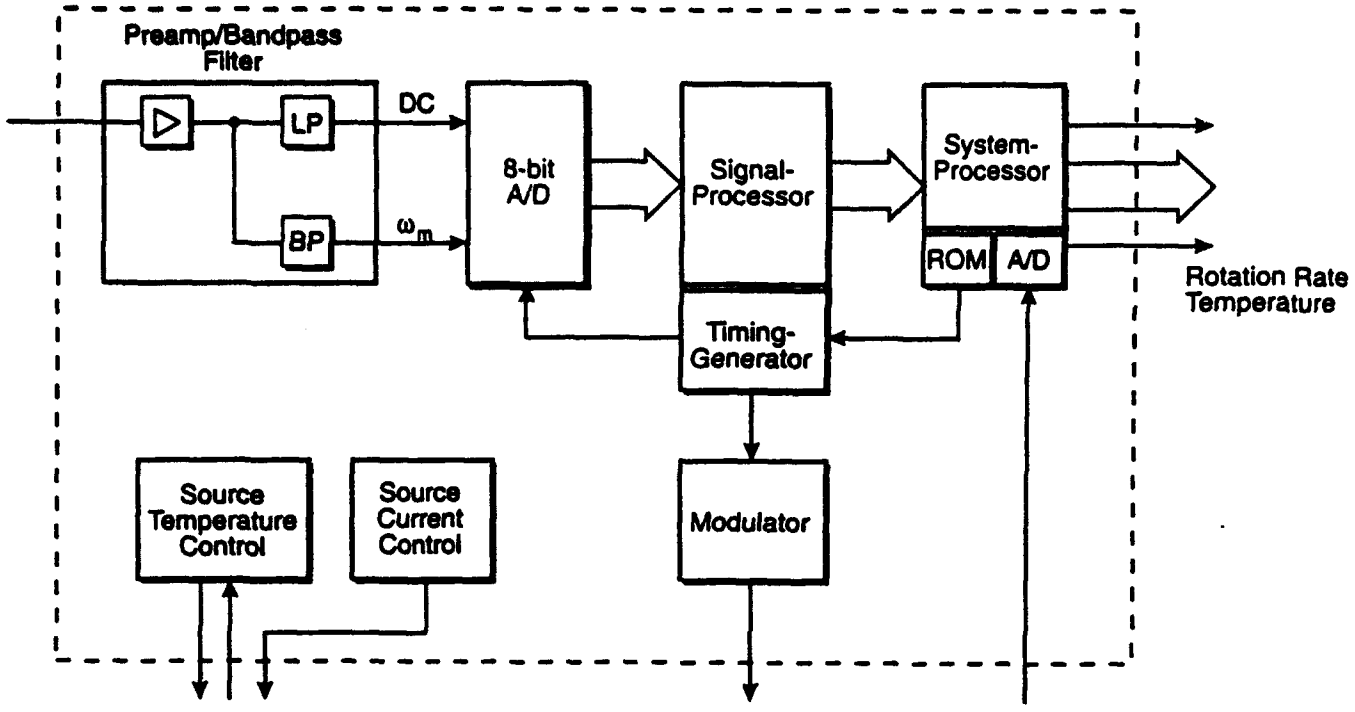

FIGURE 2: FOG Electronics

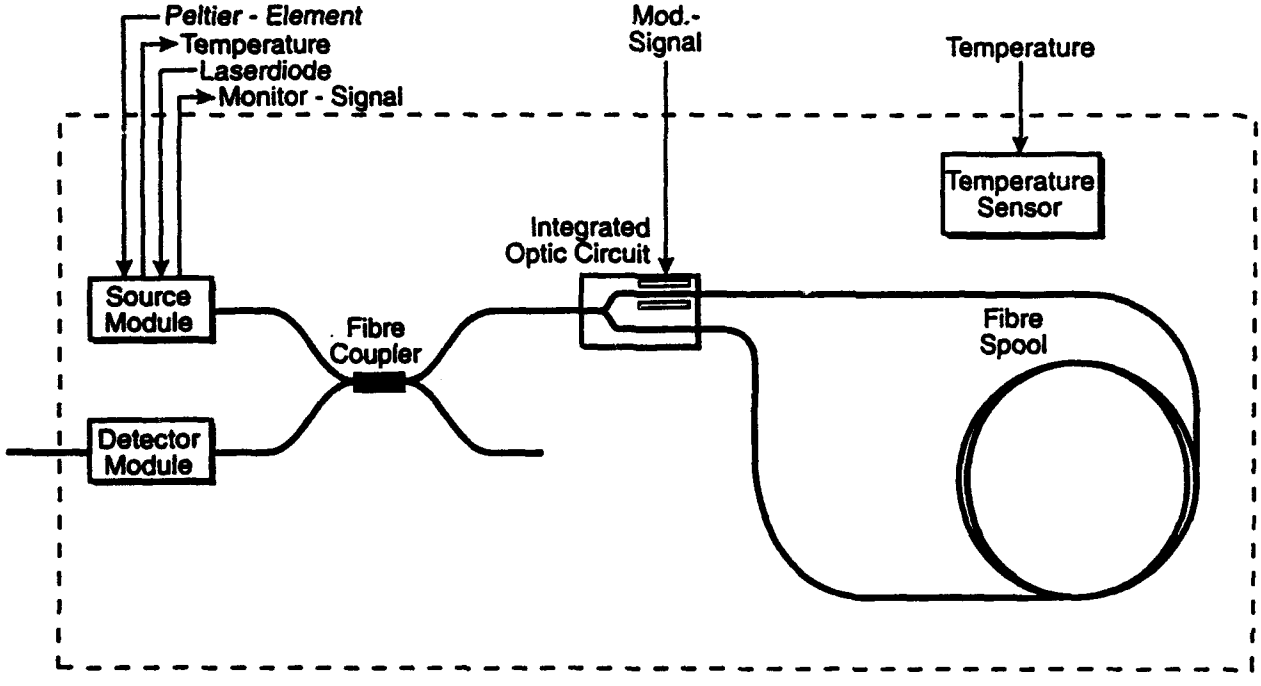

FIGURE 3: FOG Optics

OPTICS	
Diameter	80 mm
Height	26 mm
Fibre Length	100 m
Coil Radius	34 mm
Weight	400 g
ELECTRONICS	
European Standard PCB	160 mm x 100 mm
ENVIRONMENT	
Operational Temperature	-40 - +71°C
Storage Temperature	-54 - +71°C
Vibration	20-2000 Hz, 10g sine
Shock	60g/3msec, sine halfwave
PERFORMANCE	
Signal	Digital, 16-bit parallel proportional to rotation rate
Range	$\pm$ 400 deg/sec
Scale Factor	50 deg/hr/LSB
Scale Factor Error	0.5%
Bandwidth	500 Hz
Noise	10 deg/hr/$\sqrt{}$Hz
Power Dissipation	15W
DIGITAL INTERFACE	
Type	16-bit parallel Open-Collector TTL signals negative true
Sync Signal Repetition Rate	1 msec
Sync Signal Duration	1 µsec
Data valid for	800 µsec

TABLE 1: SEL FOG Performance Specification

2.0 FOG DATA OUTPUT AND RECORDING

The SEL gyro electronics provides two data output ports to the user; one is a 16-bit parallel interface providing synchronized output of the gyro rotation rate while the other is an RS-232C serial port permitting two-way communication with the gyro system processor.

2.1 Data Format

The 16-bit parallel interface provides the output for the rotation rate of the gyroscope at a repetition frequency of (nominally) 1000 Hz. The rate is represented in a two's complement format. In addition to the rate, a synchronizing signal, 'DSYN', provides the user with an indication of data validity. Details are contained in the gyroscope specifications [3].

The second ('user') interface provides for direct communication with the gyro system processor on a 9600 baud RS-232C interface. Through a series of simple commands, the user may obtain status, self-test, temperature and rate information. The data is not intended as valid gyro output information but rather for monitoring purposes and system testing. This port was monitored during laboratory testing since it provided information including sensor (gyro) temperature as well as electronics temperature. Temperature is monitored (and recorded) as a matter of course during all testing.

2.2 Hardware Interface

Data recording in the DREO Navigation Laboratory (NAVLAB) is normally performed on a PDP 11/73 computer. To interface the laboratory computer to the SEL FOG, some minor hardware adjustments had to be implemented. The FOG parallel data port output lines are supported by open-collector outputs requiring a pull up resistor on each line. An interface box containing pull up resistors for each of the data, synchronization and status lines was built. The 'DSYN' line provides a 1 μs pulse at the repetition rate of the gyro (nominally 1 KHz) which indicates that new data is available and valid for at least the next 800 μsec. This line was used to synchronize data recording. Unfortunately, due to the electrical distance between the motion simulator on which the FOG was mounted and the computer, DSYN was not capable of triggering the computer interface. A mono-stable multivibrator and a set of line drivers were used to extend the pulse width to approximately 12 μsec to support the cable length.

A table-top breakout was also provided for signal monitoring purposes. The breakout also contained a fused power switch for turning the gyroscope on and off. In particular, thermal monitoring is available at the breakout since the fixture in which the FOG was mounted was individually heated and the data monitored and recorded during all tests.

A second breakout panel is installed near the PDP 11/73 computer from where power to the table top is controlled and temperature controllers are connected.

The serial interface output from the FOG is displayed on a computer terminal and the data output lines are connected to a DRV-11 parallel line interface card in the PDP 11/73. The data received by the DRV-11 is a 16-bit two's complement number proportional to the angular rate sensed about the input axis of the FOG.

In addition, a thermal sensor is located at the base of the FOG mounting fixture. This sensor is connected to a thermometer display unit which is in turn connected to the PDP 11/73 via an IEEE-488 bus. This temperature may also be recorded along with the gyroscope rate data.

2.3 Data Recording

As noted, the data repetition rate available from the FOG is, nominally, 1000 Hz. For practical purposes, it was decided to design two separate data logging programs to permit a wide range of data logging rates [4]. These are referred to as low speed and high speed drivers. The high speed driver permits data logging at the highest input data rate (1000 Hz) while the low speed driver sums the incoming data at 1 Hz; 1000 samples are bit-wise inverted and added together in two's complement and then stored in a 32-bit buffer.

As a result, two separate data collection tasks were used during testing of the SEL FOG. Each provides for a set of user selectable parameters and dumps the data to a user specified file as well as displaying the data if desired. Each task also allows for the addition of user comments (headers) to the data files. Furthermore, a statistical data summary [5] is generated at the completion of data collection.

The slower of the two data logging programs is called LOGFOG. This routine acquires a 32-bit sum from the DRV-11 driver every 1000 FOG sample periods (an accumulation of 1000 16-bit samples). LOGFOG may then further 'block average' this data as specified by the user. The resulting data point is then an accumulation of a number (the block size) of 32-bit points which is then divided by the block size and by 1000 to get an average value for the collection period. This is referred to as block averaging. LOGFOG also provides individual time stamps on each piece of data as it is received from the driver. The time stamps are computed from the system clock. Each data point and its time stamp may be displayed and/or recorded to a data file.

The faster routine is called FSTFOG and uses the high speed DRV-11 driver to collect the 16-bit data from the FOG at the maximum rate at which it is sent on the parallel port. Up to 30,000 points may be collected in one file, corresponding to 30

The faster routine is called FSTFOG and uses the high speed DRV-11 driver to collect the 16-bit data from the FOG at the maximum rate at which it is sent on the parallel port. Up to 30,000 points may be collected in one file, corresponding to 30 seconds worth of data. Due to the speed, real-time stamps are not attached to each data point. No block averaging of the data is done. This program is particularly useful in turn-on response and rate transient analysis.

All recorded data files are post processed and plotted on laboratory PC's after test completion.

3.0 DREO TEST FACILITY

3.1 DREO Inertial Navigation Laboratory

The DREO inertial navigation laboratory was designed to be a highly versatile and flexible facility for the evaluation and development of inertial components and systems. The core of the facility is a Contraves-Goerz Model 57CD 2-axis motion simulator capable of producing and measuring highly precise position, rate and acceleration about both axes. Maximum rates of $\pm$ 1000 deg/sec are possible.

Data acquisition and table control are accomplished through a PDP-11/73 computer via IEEE-488 interfaces to all instrumentation.

A photograph of the laboratory is shown in Figure 4.

Details on test equipment and laboratory capabilities are contained in DREO Report # 895. [6]

3.2 Test Fixturing and Alignment

Figure 5 shows the SEL FOG in its mounting fixture on the top of the motion table. The fixture contains heaters for precise temperature control and a resistance thermometer (RTD) for temperature monitoring and recording. The grey box beside the gyro contains the pull-up resistors and line driver circuitry. The black box is the FOG electronics and the table top breakout is beside it.

Gyroscope alignment was performed using precision bubble levels to align the fixture to the table top. More precise alignment is not possible (or necessary) due to the high noise level as seen at the output of the gyro.

Temperature of the gyroscope was controlled to $\pm$ 0.1° Celsius.

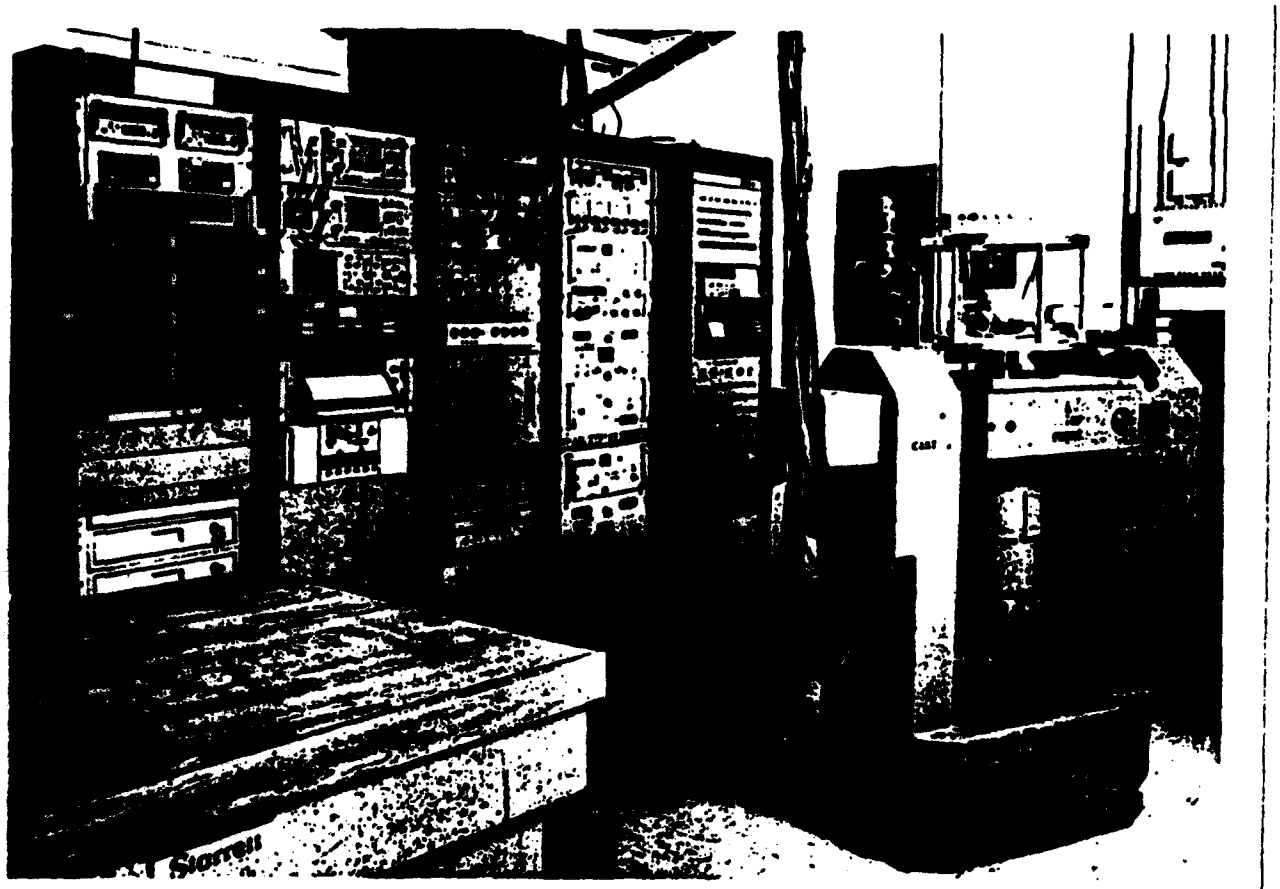

FIGURE 4: DREO Inertial Navigation Laboratory

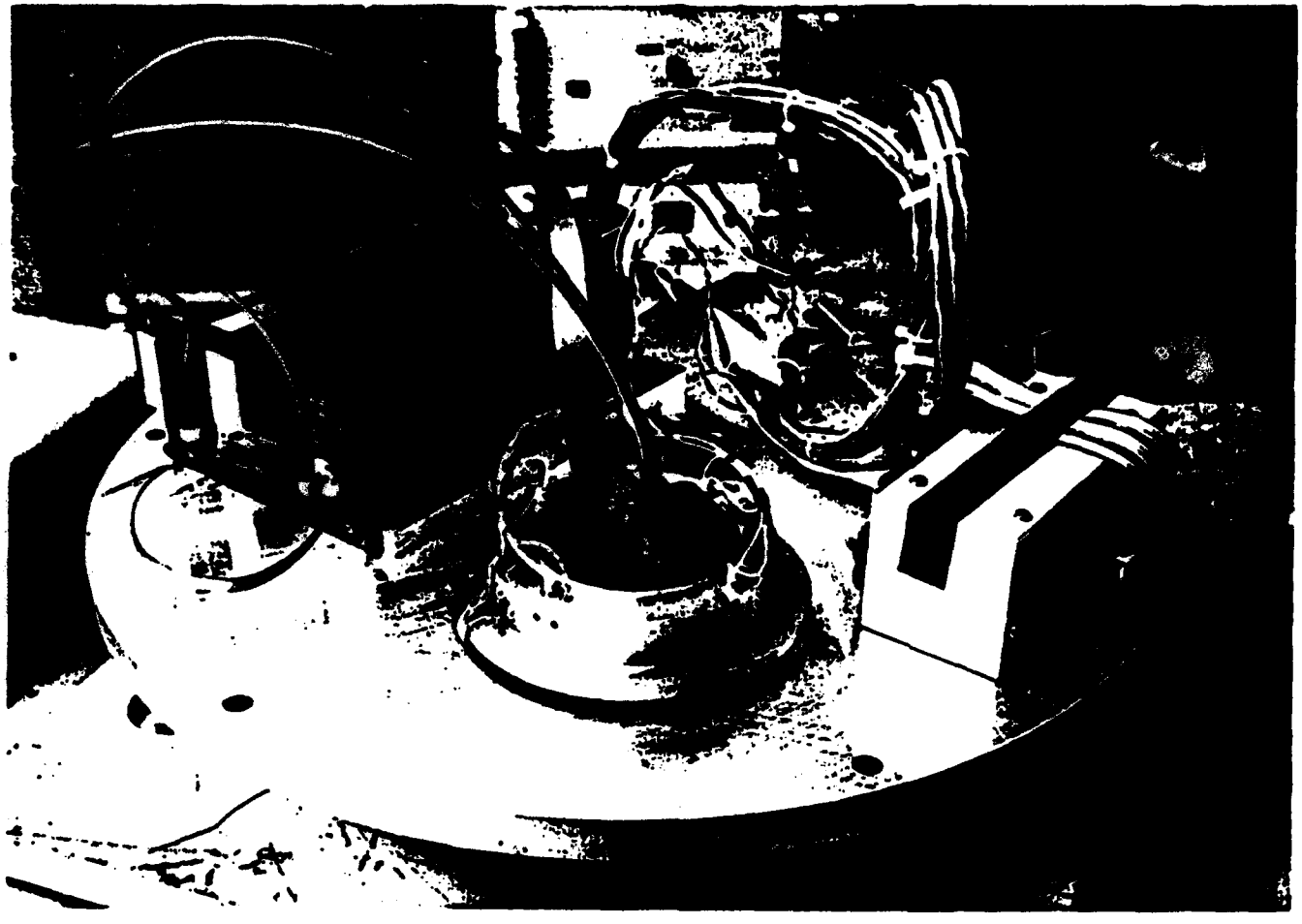

FIGURE 5: SEL FOG Mounted on Test Table

4.0 TEST PROGRAM

4.1 Historical

A Fibre Optic Gyroscope is tested in much the same manner as the Ring Laser Gyroscope to determine sensor error terms. The terms of interest include the magnitudes of the bias drift (BD) and scale factor (SF) and their transient responses to turn-on, sensitivity to temperature change and gradients, stability and day-to-day repeatability. A typical series of tests is shown in Table 2 [1].

I. WARM-UP TIME	hr
II. BIAS	
- magnitude	deg/hr
- turn-on transient	deg/hr
- stability	deg/hr
- day to day reapeatability (across turnoffs, cooldowns and thermal variations	deg/hr
- transient with thermal change	deg/hr
- repeatability	deg/hr
III. SCALE FACTOR	
- magnitude (at ambient and other temperatures)	arcsec/count
- turn-on transient (amplitude and time constant)	ppm
- stability (over temp. and rate)	ppm
- day to day repeatability (across turnoffs, cooldowns and thermal variations)	ppm
- linearity (deviation) with rate (at various temperatures)	ppm
- transient with thermal change	ppm
- repeatability	ppm

TABLE 2: FOG Tests

Bias drift and scale factor are defined by the following:

Bias drift (determined with motion table stationary)

$$BD = \frac{N_o}{\Delta t} SF_N - \varpi \quad \text{deg/hr}$$

where N_o = Net gyro output pulses with the table stationary
Δt = sample time
SF_N = nominal scale factor
ϖ = local component of earth rate

and

Scale factor (determined with table rotating)

$$SF = \frac{R}{N \pm \frac{\Delta t\,(BD + \varpi)}{SF_N}} \quad \text{deg/hr/count}$$

where

N = Net gyro output pulses with table rotating
R = rate of rotation

Note that the units of scale factor can be expressed in several ways; digital output format is, typically, a pulse corresponding to the minimum angle that can be resolved by the photodetector circuit, i.e. arc seconds (or degrees) of rotation/pulse. The resultant pulses are then accumulated in a counter over a given sample period (the SEL FOG provides the accumulated pulse count at 1000 Hz or every 0.001 seconds). The SEL FOG provides this count as a 16-bit data word. Under this mechanization, scale factor is expressed in deg/hr/LSB (least significant bit) which combines the resolution of the detector (arcsec or degrees per pulse) with the output rate (in seconds or hours) but, in the end, is limited by the dynamic range of the digital data word (16 bits).

For the SEL FOG, the rate range is approximately $\pm$450 deg/sec. For a 16-bit data word, the resolution of the least significant bit (LSB) then becomes $\approx$ 50 deg/hr: hence, the nominal scale factor for this gyro is expressed as $\approx$ 50 deg/hr/LSB.

4.2 Test Procedures

Section 2.3 describes the data recording capabilities developed to facilitate testing of the SEL FOG. To complete the tests as listed in Table 2, a logical sequence of test procedures was developed employing the various data recording options. A complete series of tests was first carried out at gyro operating temperature of (nominally) 30°C. A typical test sequence consisted of:

a) turn-on transient test during which the gyro was turned on having been preheated and stabilized at 30°C. Data was recorded at 1KHz for 10 seconds.

b) bias drift tests during which data was recorded at 1 second or 180 second block averaged intervals for 1 to 60 hours. Numerous repetitions of these drift tests provided bias repeatability data and longer tests (up to 60 hours) provided stability data and were also used in rate cluster analysis, to be described below.

c) scale factor tests during which input (table) rate was varied from -400 to +400 deg/sec in sequential steps. Scale factor at each rate was determined from the highly precise motion table rate.

d) scale factor stability tests during which the gyro was subjected to a 100 deg/sec input rate for extended periods of time ranging from 1 to 16 hours. Resulting data provided thermal settling time and scale factor stability data.

The above series of tests was then repeated at nominal gyro operating temperatures of 40°C and 50°C to determing thermal sensitivity of bias and scale factor.

In addition thermal transient tests were conducted where temperature was varied (under operator control) from 30°C to 50°C and vice versa.

A complete list of tests performed on SEL FOG model PM1DE, serial number 88/00021 is contained in Table 3. File names are coded to contain test type and date of test as follows:

Filename = AAXXXYYB.CDE

where: AA denotes type of test
i.e. BD denotes bias draft
RP denotes rate pulse
RS denotes rate stability
RT denotes rate transient
SF denotes scale factor
TT denotes thermal transient

XXX denotes Julian day of year
(1-366)

YY denotes year (92, 93, etc.)

B denotes test sequence performed on a given day
(A = 1st test, B = 2nd test, C = 3rd test)

.CDE is the file extension
(.FOG = gyro data file, .TMP = temperature file, .TBL = table rate file)

FILE	TEMP.°C	SAMPLE RATE	DURATION
BD34992A.FOG	30	180 Sec (.0056 Hz)	16 Hr
BD35092A.FOG	30	1 Hz	1 Hr
BD35692A.FOG	30 - CS	1 KHz	30 Sec
BD35792A.FOG	30 - CS	1 KHz	5 Sec
BD00493A.FOG	30 - CS	1 KHz	10 Sec
BD00493B.FOG	30	1 Hz	1 Hr
BD00493C.FOG	30	1 KHz	10 Sec
BD00493D.FOG	30	100 Sec (.01 Hz)	6 Hr
BD00693A.FOG	40 - CS	1 KHz	10 Sec
BD00693B.FOG	40	1 Hz	1 Hr
BD00693C.FOG	40	1 KHz	5 Sec
BD00693D.FOG	40	100 Sec (.01 Hz)	8 Hr
BD00693E.FOG	40	1 KHz	10 Sec
BD00893B.FOG	50	30 Sec (.033 Hz)	60 Hr
BD01193A.FOG	50 - CS	1 KHz	10 Sec
BD01193B.FOG	50	1 KHz	10 Sec
BD01193C.FOG	50	1 Hz	1 Hr
BD01193D.FOG	50	1 KHz	7 Hr
BD01593A.FOG	30	30 Sec (.033 Hz)	60 Hr
BD01593A.FOG	30	30 Sec (.033 Hz)	60 Hr
RP36592A.FOG	30	1 KHz	10 Sec
RP36592B.FOG	30	1 KHz	10 Sec
RP01393A.FOG	30	180 Sec (.0056 Hz)	15 Hr
RS35092A.FOG	30	180 Sec (.0056 Hz)	15 Hr
RS35092A.TBL	30	180 Sec (.0056 Hz)	16 Hr
RS3529A.FOG	30	180 Sec (.0056 Hz)	16 Hr
RS3529A.TMP	30	180 Sec (.0056 Hz)	16 Hr
RS35692A.FOG	30	180 Sec (.0056 Hz)	16 Hr

TABLE 3: FOG Data File Index (SEL FOG S/N 88/00021)
LEGEND: BD - Bias Drift, RP - Rate Pulse, RS - Rate Stability, CS - Cold Start

FILE	TEMP.°C	SAMPLE RATE	DURATION
RS35692A.TMP	30	180 Sec (.0056 Hz)	16 Hr
RS35792A.FOG	30	180 Sec (.0056 Hz)	24 Hr
RS35792A.TMP	30	180 Sec (.0056 Hz)	24 Hr
RS36692A.FOG	30	1 KHz	10 Sec
RS36692B.FOG	30	1 Hz	1 Hr
RS36692C.FOG	30	100 Sec (.01 Hz)	7 Hr
RS00793A.FOG	40 - Ton	1 KHz	10 Sec
RS00793B.FOG	40	1 KHz	10 Sec
RS00793C.FOG	40	1 Hz	1 Hr
RS00793D.FOG	40	100 Sec (.01 Hz)	7 Hr
RS01293A.FOG	50	1 KHz	10 Sec
RS01293B.FOG	50 - Ton	1 KHz	10 Sec
RS01293C.FOG	50	1 Hz	1 Hr
RS01293D.FOG	50	100 Sec (.01 Hz)	7.5 Hr
RT35692A.FOG	30	1 Hz	6 Sec/Rt
RT35792A.FOG	30	30 Sec (.033 Hz)	5 Min/Rt
SF34692A.FOG	30	180 Sec (.0056 Hz)	15 Min/Rt
SF34692B.FOG	30	180 Sec (.0056 Hz)	15 Min/Rt
SF36492A.FOG	40	180 Sec (.0056 Hz)	15 Min/Rt
SF36592A.FOG	40	180 Sec (.0056 Hz)	15 Min/Rt
SF00793A.FOG	50	180 Sec (.0056 Hz)	15 Min/Rt
SF01193A.FOG	50	180 Sec (.0056 Hz)	15 Min/Rt
SF01293A.FOG	50	180 Sec (.0056 Hz)	15 Min/Rt
TT01393A.FOG	30 → 50	100 Sec (.01 Hz)	14 Hr
TT01393A.TMP	30 → 50	100 Sec (.01 Hz)	14 Hr
TT01493A.FOG	50 → 30	100 Sec (.01 Hz)	7 Hr
TT01493A.TMP	50 → 30	100 Sec (.01 Hz)	7 Hr
TT01493B.FOG	30 → 50	100 Sec (.01 Hz)	16 Hr
TT01493B.TMP	30 → 50	100 Sec (.01 Hz)	16 Hr
TT01593A-FOG	50 → 30	100 Sec (.01 Hz)	7 Hr
TT01593A-TMP	50 → 30	100 Sec (.01 Hz)	7 Hr

TABLE 3: FOG Data File Index (Continued)
LEGEND: RT-Rate Transient, SF-Scale Factor, TT-Temperature Transient

5.0 TEST RESULTS

5.1 Data Reduction

The raw data files recorded on the DEC PDP 11/73 are transferred to the DOS environment by means of a Kermit routine. The data is then reduced, plotted and statistical results determined using BBN software application RS/1.

Data logged during the FOG testing included Time, FOG Rate Output (LSB), Temperature, and Table Rates.

Scale factor and scale factor error were calculated from the raw data files as follows:

$$SF = Tbl_{rt} \text{deg/sec} \times 3{,}600 \text{ sec/hr} / (\text{FOG Output (LSB)} - \text{Bias (LSB)})$$

$$SF_{error} = (SF - SF_{mean})/SF_{mean} \times 100\%$$

where SF - Scale Factor, deg/hr/LSB
LSB - Least Significant Bit
TBl_{rt} - Table Rate, deg/sec

5.2 Rate Cluster Analysis

Cluster analysis (or the 'cluster sampling technique') is a data analysis method used to measure output stability of an oscillator in the time domain [7]. In this case, the FOG is the oscillator. The technique provides a set of characteristics that are directly comparable between data sets which may use varying integration periods for the collection of data and is used to characterize various types of noise terms in the gyro data by performing several simple operations on the entire data set.

Cluster analysis is performed by scanning a moving window across the acquired gyro data set [8]. The data set within the window is called a cluster. The time average of the data points in each cluster is calculated and then the differences between each two adjoining clusters is determined. These differences become a new set of random variables whose variance is called the 'cluster variance'.

This procedure is repeated for other cluster sets for windows of different lengths and the square root of the resulting cluster variances are plotted against time (cluster length). The result is a characteristic curve whose shape is determined by various error terms in the data. References [7] and [8] provide a detailed explanation and derivation of the technique.

The error terms of significance to us include the angular random walk (defined as the growth in angular error with time due to white noise in the angular rate) expressed in units of deg/$\sqrt{}$hr and bias instability (low frequency noise) expressed in deg/Hr. [9]

Additionally, one may extract the rate random walk (defined as drift rate error growth with time due to white noise in angular acceleration).

A detailed description of the specific procedures employed in the cluster analysis of the SEL FOG data is contained in Ref [10].

5.3 Presentation of Results

5.3.1 Turn-On Transient

Figure 6 is a plot of gyro turn-on at 30°C with sampling at 1 KHz for 10 seconds. The first 200 msec of the data are plotted and indicate a turn-on time of 20-25 msec. Figure 7 shows the same data file but includes all 10 seconds of data. After turn-on, the gyro indicates no further immediate transients and can be considered functional.

5.3.2 Bias Drift/Bias Stability/Bias Repeatability

Tests of varying lengths ranging from one to sixty hours were conducted at a gyro temperature of 30°C. A list of the bias drifts is shown in Table 4. At 30°C, the mean bias drift was determined to be *5.38 deg/hr with a repeatability of* $\pm$ *0.68 deg/hr.*

Figure 8 is a 60 hour bias drift test conducted at 30°C with block averaging over 30 seconds per sample. The lower plot shows the bias drift while the upper plot is gyro temperature. The sinusoidal variations in temperature are due to cyclic room temperature variations. Thermal sensitivity will be discussed in detail in the following sections. Aside from limited thermal tracking, the bias drift remains almost constant with a bias stability of 1.16 deg/hr (1 σ). (Bias stability is the standard deviation of the bias over the whole data set).

Figures 9 and 10 illustrate several points of interest. Both are bias drift tests at 30°C; Figure 9 is sampled at 1 Hz for 60 minutes while Figure 10 is at 0.01 Hz for 6 hours. The mean bias drift in Figure 9(a) is 6.10 deg/hr $\pm$ 5.61 deg/hr (1σ) and in Figure 10(a) is 5.56 deg/hr $\pm$ 0.56 deg/hr (1σ). Figure 10(b) illustrates the improvement in noise reduction due to the longer integration period.

0 FILE	1 TEMP [C]	2 SpltRt [S]	3 Bias Dft [Deg/Hr]
1 SFL36492A	30	180	4.6973
2 SFL36492A	30	180	5.5271
3 SFL36492A	30	180	5.7871
4 SFL36592A	30	180	5.3421
5 SFL36592A	30	180	5.0872
6 SFL36592A	30	180	5.3521
7 SFL00693A	40	180	1.4429
8 SFL00693A	40	180	0.8730
9 SF00693A	40	180	1.0180
10 SFL00793A	40	180	1.2580
11 SFL00793A	40	180	1.3030
12 SFL00793A	40	180	1.1430
13 SFL01193A	50	180	-12.5490
14 SFL01193A	50	180	-12.6290
15 SFL01193A	50	180	-13.4040
16 SFL01293A	50	180	-13.1790
17 SFL01239A	50	180	-13.8340
18 SFL01293A	50	180	-12.9990
19 BD00493D	30	100	5.5570
20 BD01493A	30	30	5.7011
21 BD00693D	40	100	1.5923
22 BD00893A	50	30	-9.0400
23 BD00893B	50	30	-11.5300
24 BD01193D	50	100	-11.890

TABLE 4
Mean @ 30°C, Mean @ 40°C, Mean @ 50°C

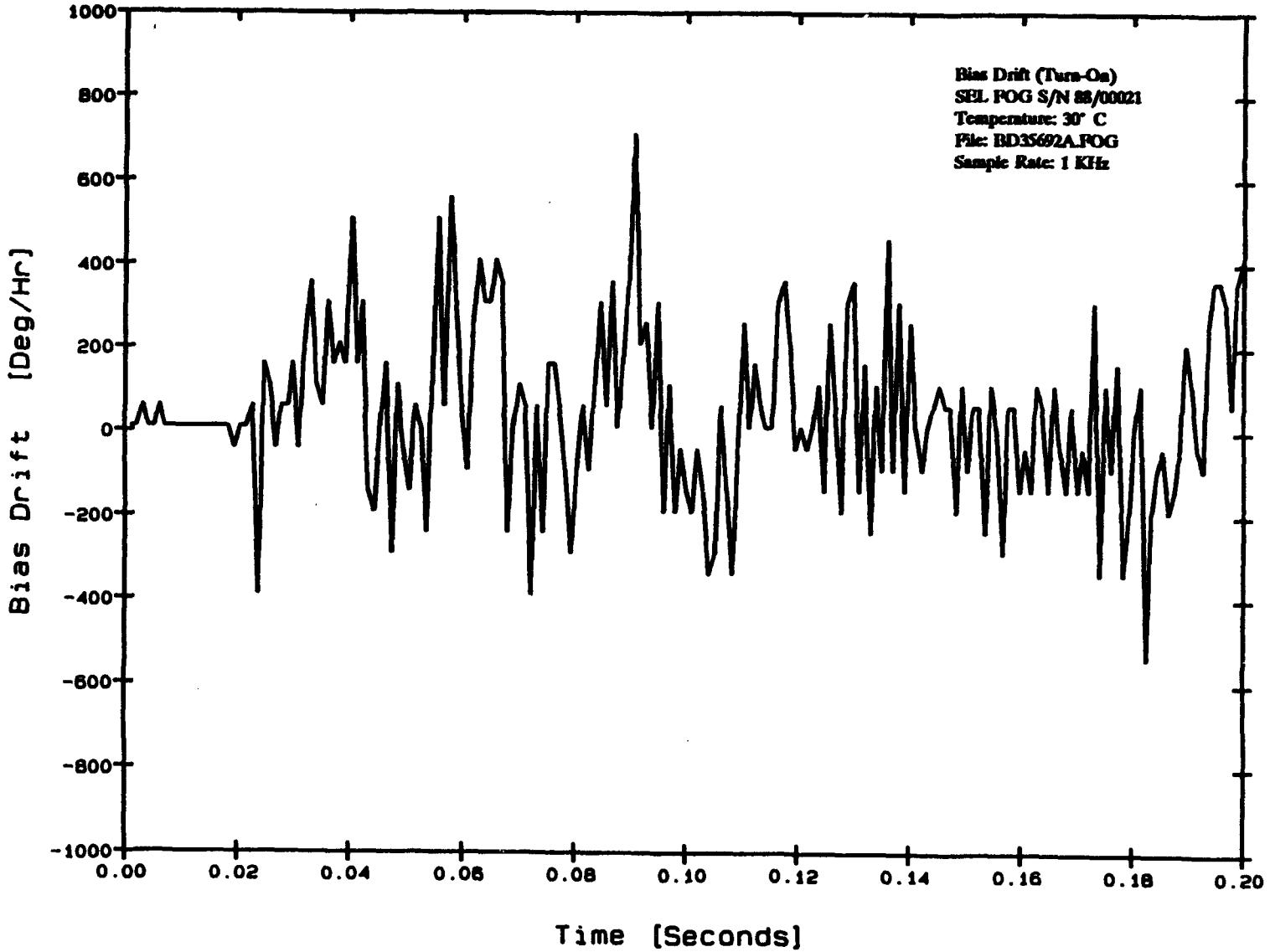

FIGURE 6: Gyro Turn-On at 30^{O}C

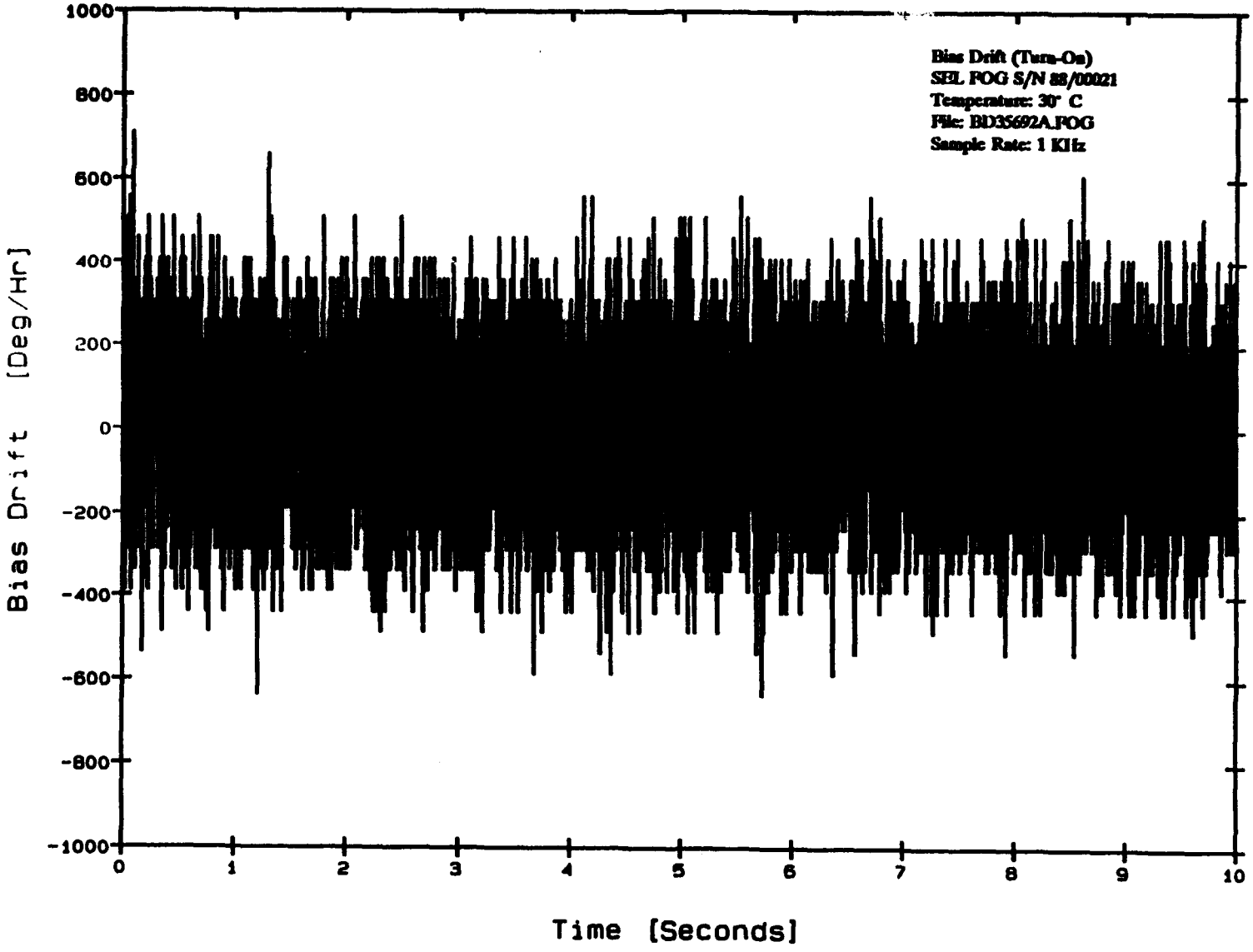

FIGURE 7: Gyro Turn-On

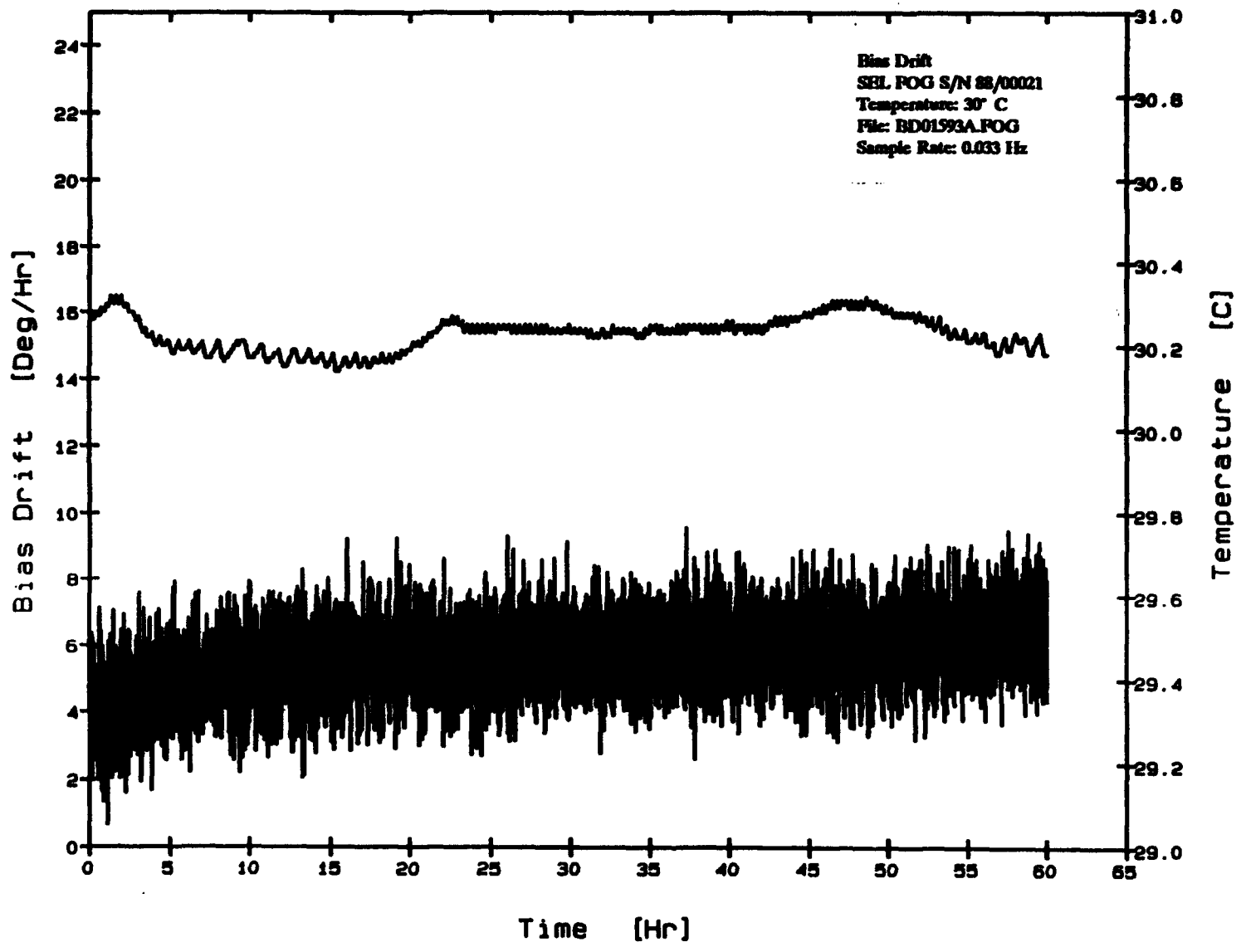

FIGURE 8: 60-Hour Bias Drift Test

FIGURE 9(a): Bias Drift, 1 Hz

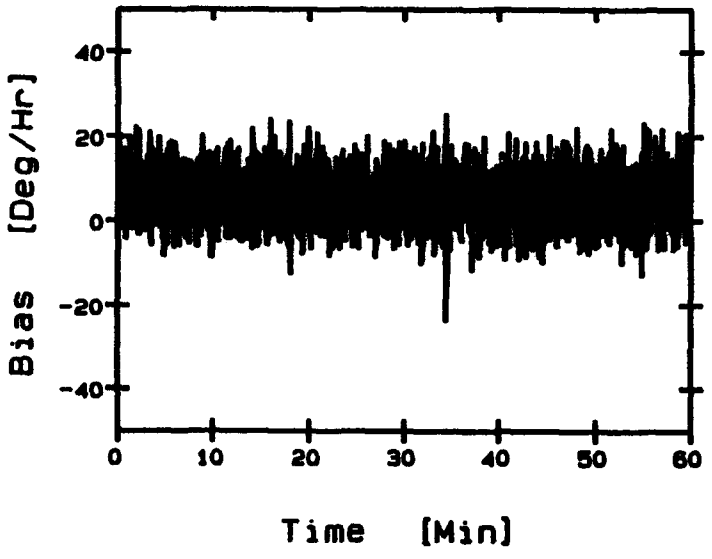

FIGURE 9(b): Bias Drift, 1 Hz

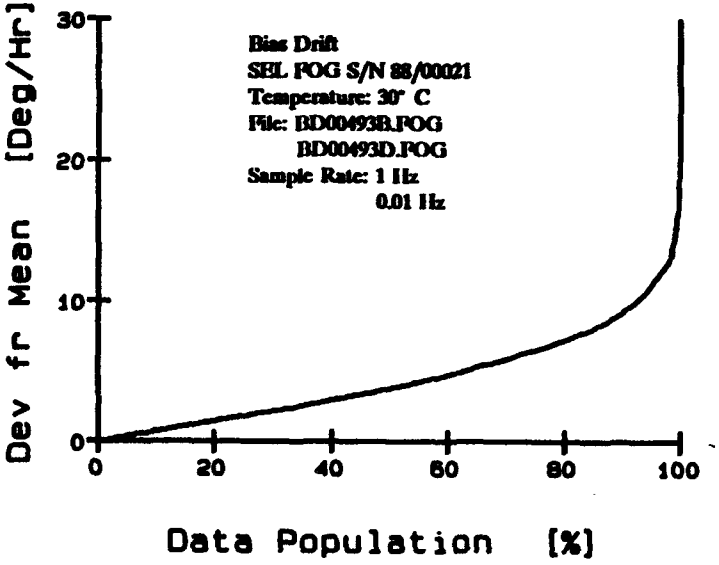

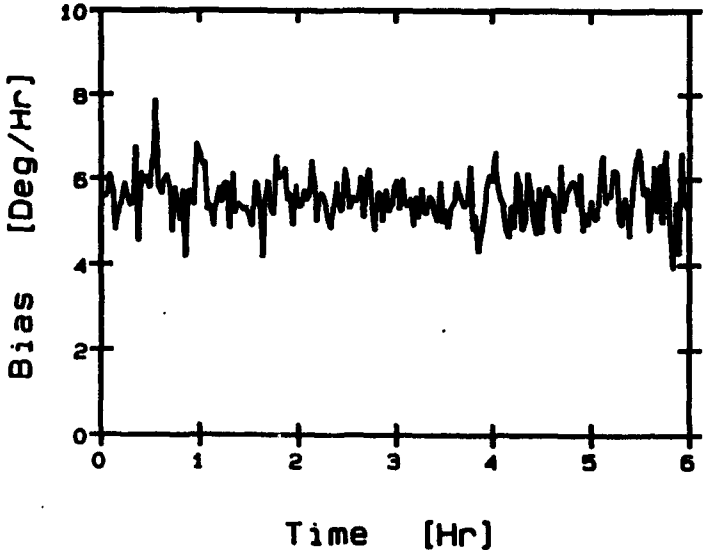

FIGURE 10(a): Bias Drift, 0.01 Hz

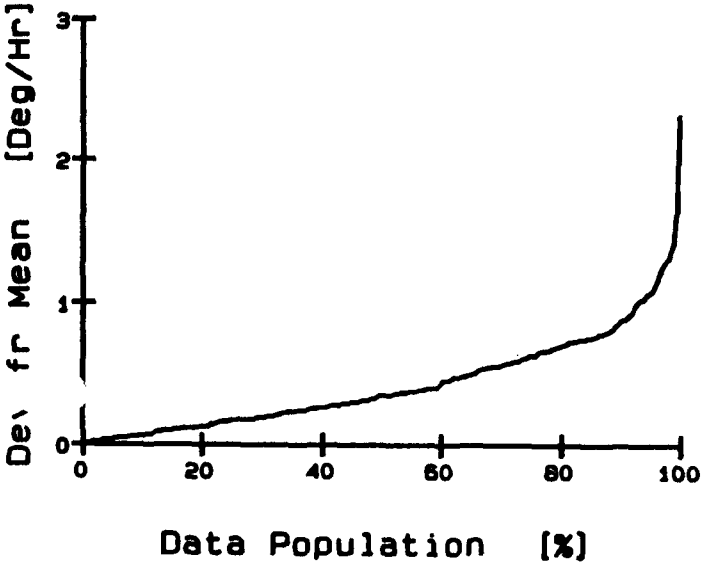

FIGURE 10(b): Bias Drift Deviation, 0.01 Hz

A cluster analysis was then performed on a 60 hour data file, BD01593A, shown previously in Figure 8. Figure 11 shows this bias drift data again. The file consists of 7078 data points accumulated using a 30 second block averaging (integrating) period. Earth rate is removed from the rate data and scaling is accomplished using a nominal scale factor of 49.99 deg/hr/LSB following the procedures as documented in Ref [10] and [7], the gyro data file is processed through a rate cluster analysis program which computes the mean bias and bias drift of the set of clusters whose lengths vary from one sample point to the maximum possible cluster length of one-third of the total number of sample points in the file. The result is a file containing cluster period, variance, standard deviation and tabulated error for each cluster length.

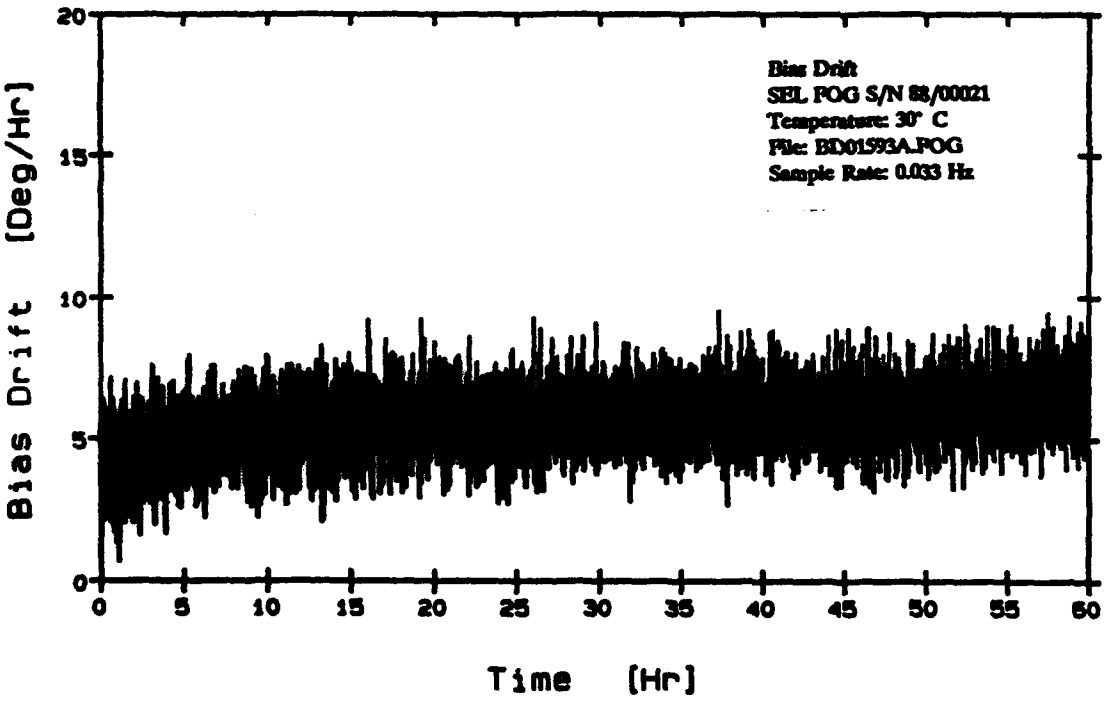

FIGURE 11: SEL FOG Bias at 30°C for 60 Hour Test (Corrected for local earth rate).

Figure 12 is a plot of the mean bias for each hour of the 60 hour test in Figure 11. The bias stability of 0.56 deg/hr is the standard deviation of the set of hourly mean biases.

Figure 13 is the rate cluster plot of the data set in Figure 11. In rate cluster analysis, the calculated cluster standard deviation is plotted against cluster period in a Log-Log format. The noise terms (angular random walk, bias instability and rate random walk) as well as an error estimate of each term are taken directly from the plot.

By definition, a -0.5 slope line fitted to the first part of the curve and extended to the 2-hour cluster period intercept, provides an estimate of Angular Random Walk (ARW). In this case the ARW is $0.11 \pm 6.5\%$ deg/$\sqrt{\text{Hr}}$. Bias Instability (low frequency noise) is determined by fitting a zero-slope line to the bottom (local) minimum point on the curve and extending it to the vertical axis. The Bias Instability is $< 0.14 \pm 12.5\%$ deg/hr. Note that bias instability is not to be confused with bias stability; although the terms appear similar, bias instability is a purely statistical term relating to the level of low frequency noise in a given data set and is only useful for comparison of various data sets. Bias stability on the other hand is an absolute gyroscope performance-related term defined as the deviation in gyroscope bias drift over a given data set.

As shown in reference [7] Rate Random Walk, determined from the rate cluster analysis plot by fitting a line with slope +1/2 to the right hand tail end of the curve and extending it to a cluster period of 1.5 hours, is difficult to determine from this plot although some evidence of Rate Random Walk exists. A rate cluster analysis performed on another data set taken at a gyro temperature of 50°C illustrates a more distinct Rate Random Walk and will be discussed in the following section dealing with bias temperature sensitivity.

As previously noted, temperature variation and stability during these tests is of concern, particularly due to the apparent upward bias trend over the first 20-25 hours of the test. During the test, both room (ambient) temperature and FOG block temperature were recorded. Figure 14 is a plot of both data sets. The data shows a mean gyro temperature of 30.23°C with a stability of 0.04°C (1σ). The peak-to-peak variation is less than 0.2°C over the entire 60 hour test. The laboratory ambient temperature averaged 20.6 ± 0.5°C with a peak to peak range of 2°C. This is typical in the DREO Navigation Laboratory. The temperature sensitivity of this FOG will be further explored in the following section.

5.3.3 Bias Temperature Sensitivity

Table 4 in the previous section illustrated the bias drift determined for all tests conducted and includes tests at 30°C, 40°C and 50°C. As stated, the bias drift at 30°C was determined to be 5.38 deg/hr with a repeatability of $\pm$ 0.68 deg/hr. Similarly, from Table 4, bias drift at 40°C is 1.23 deg/hr with a repeatability of $\pm$ 0.36 deg/hr and at 50°C is -12.34 deg/hr with a repeatability of $\pm$ 3.3 deg/hr. This data is plotted in Figure 15. From this plot, it is evident that bias drift temperature sensitivity is not linear.

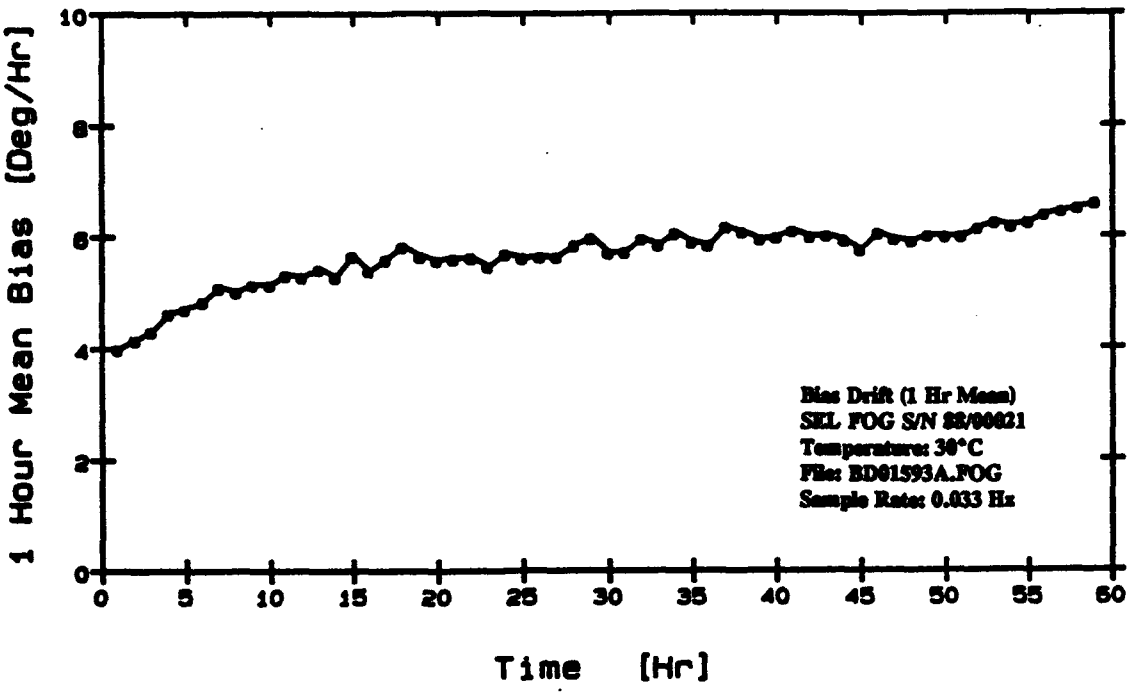

FIGURE 12: Means Biases for each hour of 30°C Drift Test

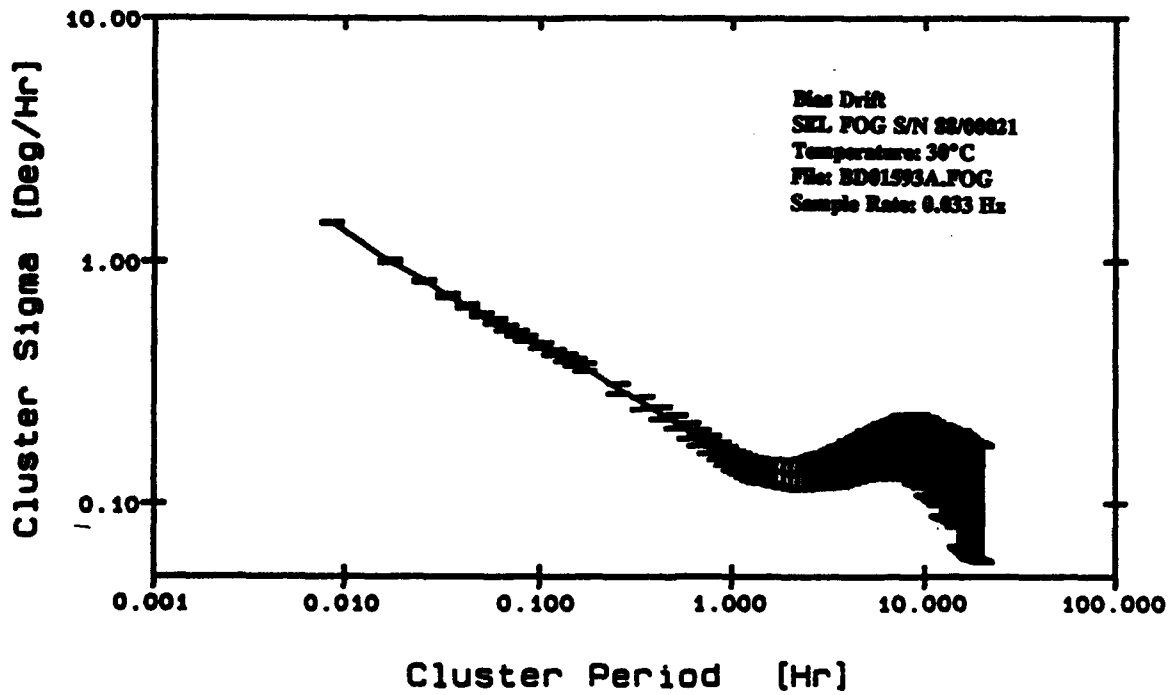

FIGURE 13: Rate Cluster Analysis at 30°C

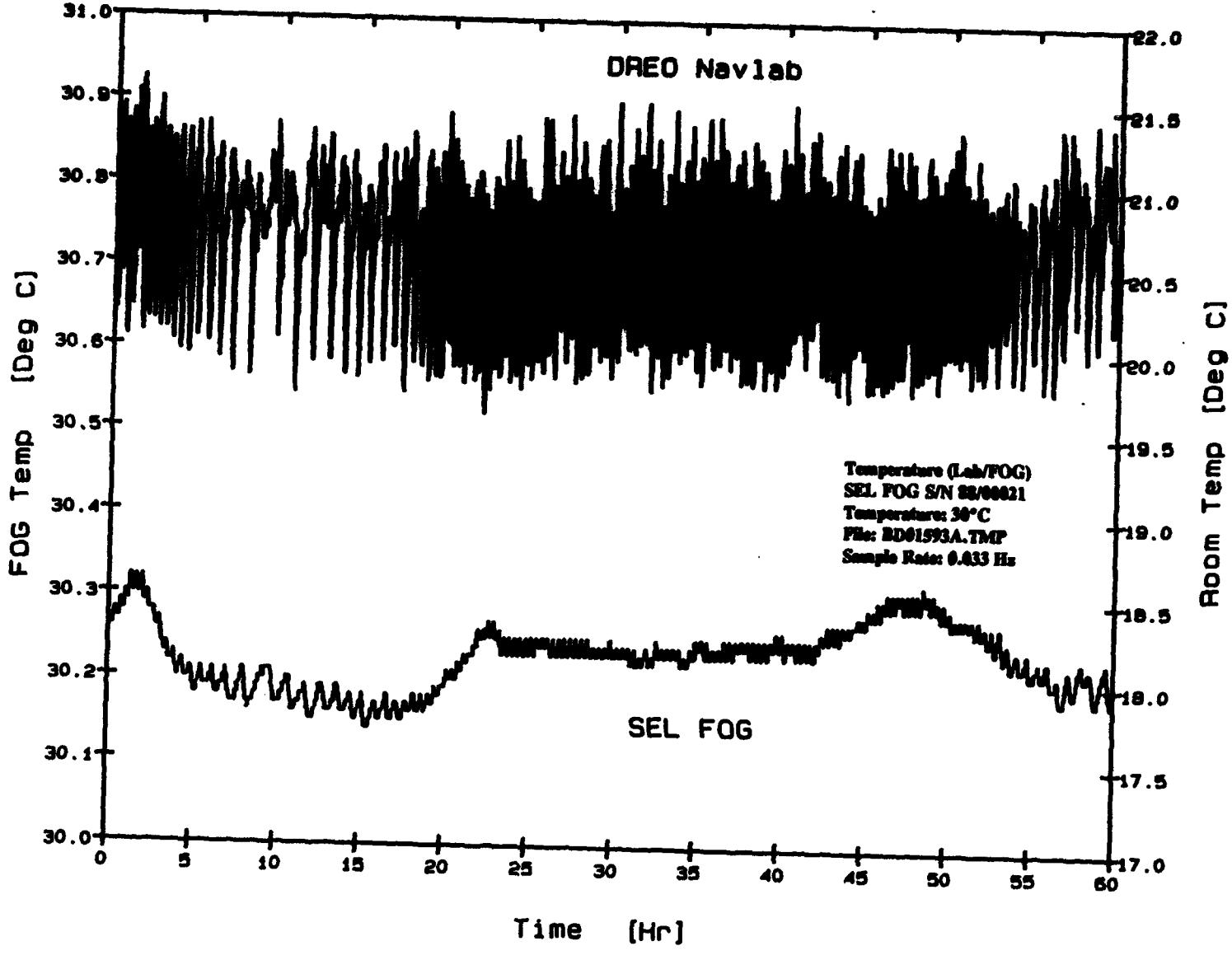

FIGURE 14: Temperature during 60 hours Drift Test

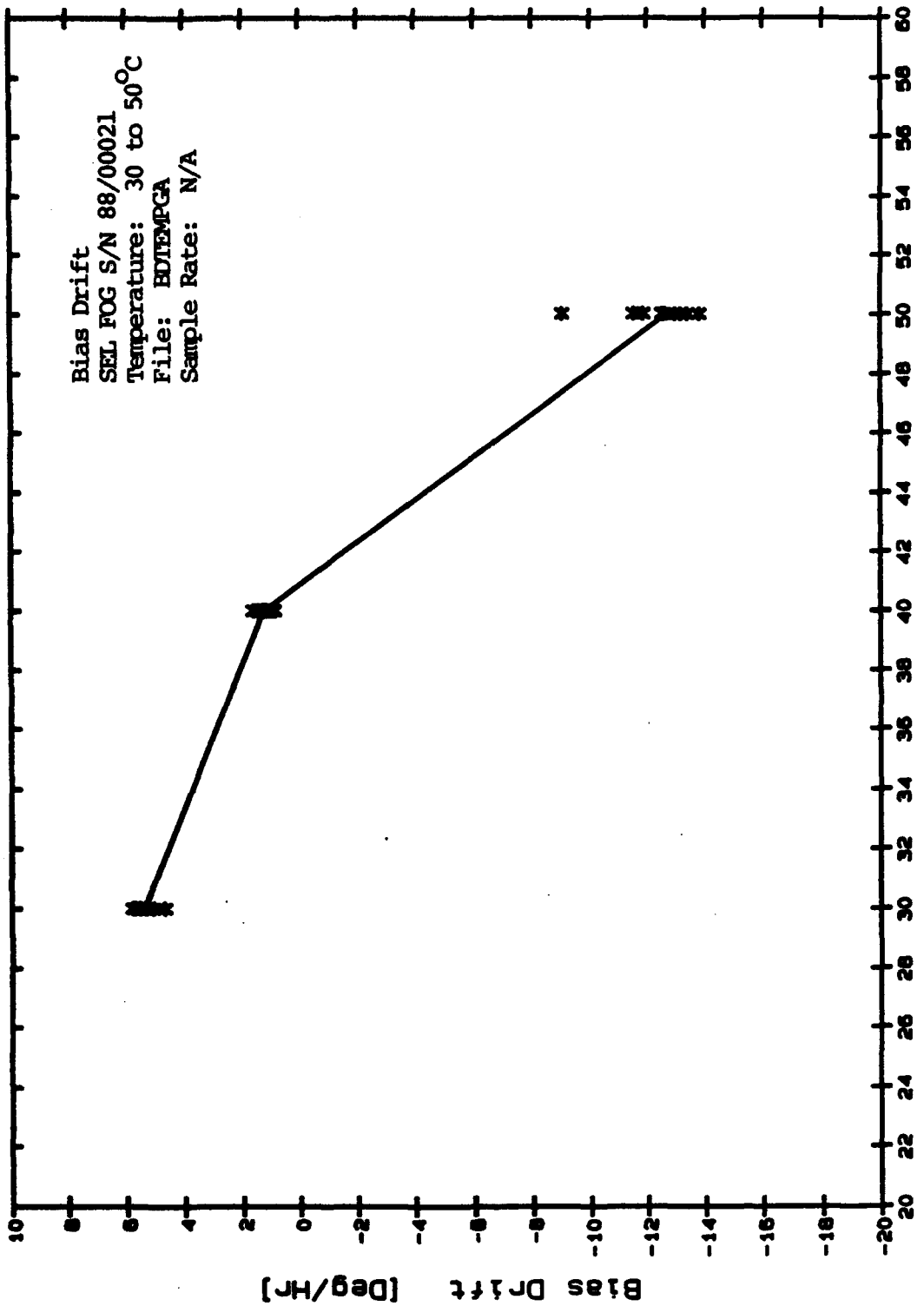

FIGURE 15: Bias Temperature Sensitivity

The effects of thermal transients are also of interest. According to the manufacturer's documentation, the SEL FOG electronics performs thermal compensation of the gyroscope output rate. No specifics on how the compensation is implemented are available. The effects of thermal transients are of significance since, in most applications, the gyros would be unheated and, therefore, exposed to the effects of thermal transients due to turn-on (illustrated and discussed in the previous section) as well as temperature changes in the ambient environment. This latter effect was simulated by applying controlled thermal transients to the gyro after turn-on and settling. The results of one such series of tests are illustrated in Figure 16. Figure 16(a) shows a 30°C to 50°C temperature change while Figure 16(b) shows a 50°C to 30°C change. The maximum rate of change of temperature is ≈ 2°C/min for the first test and 0.6°C/min for the second test. Note the bias drift transient. In the first case (Fig. 16a) the gyro bias undergoes a dramatic transient as the temperature increases, starting at ≈ 3.0 deg/hr and then peaking at over 70 deg/hr before recovering and finally settling at ≈ -12.0 deg/hr. Similarly in the second test (Fig 16b) the bias goes from ≈-12.5 deg/hr at 50°C through a transient peaking at ≈-50 deg/hr and then settling to ≈3.0 deg/hr, as before.

These extreme transients seem to indicate an inability on the part of the FOG thermal compensation to track sudden temperature transients. In both cases, as the rate of temperature transient decreased, the gyro recovered and settled to nominal bias drift values for the given temperature.

For comparison purposes, a second rate cluster analysis was also performed on a data set taken at a gyroscope temperature of 50°C. From this, the effects of temperature on angular random walk, bias instability and rate random walk can be determined. Again, a 60 hour bias drift test was run with samples taken at a 30 second integration period for a total of 7200 samples as shown in Figure 17. The lower plot illustrates the raw gyro rate data with earth rate removed and scaled using a nominal scale factor of 49.99 deg/hr. Note, again, the settling trend of the data over the first 25-30 hours. Again, this can be attributed to thermal effects and settling. The upper plot shows the mean bias for each hour of data in the test and clearly illustrates the thermal transient. Bias drift for the raw data set is -11.53 deg/hr with a stability of $\pm$ 1.34 deg/hr (1σ), agreeing with the data in Figure 15 for a temperature of 50°C.

Using the cluster analysis techniques, and the rate cluster plot shown in Figure 18 we can determine the angular random walk to be 0.094 deg/$\sqrt{\text{Hr}}$ $\pm$ 6.5% and the bias instability to be 0.16 deg/hr $\pm$ 12.5%; both in very close agreement with the results at 30°C. In this case, though, there is also some clearer evidence of rate random walk. The rate random walk is 0.12 deg/hr/$\sqrt{\text{hr}}$ $\pm$ 22%. This would seem to indicate that at higher block temperatures, the white noise processes within the gyro become such that a rate random walk becomes an apparently significant factor. In fact, the evidence may suggest that the observed change in bias with temperature may be due to the growth of the rate random walk term under these conditions.

FIGURE 16(a): Thermal Transient 30-50°C

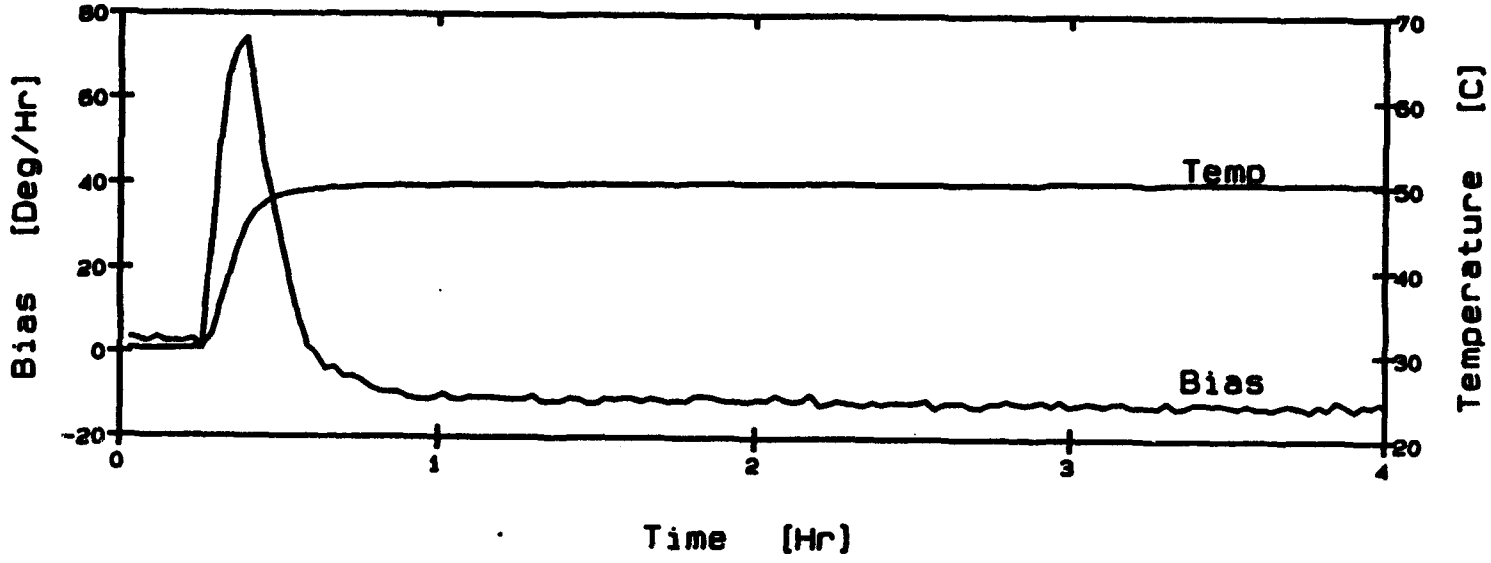

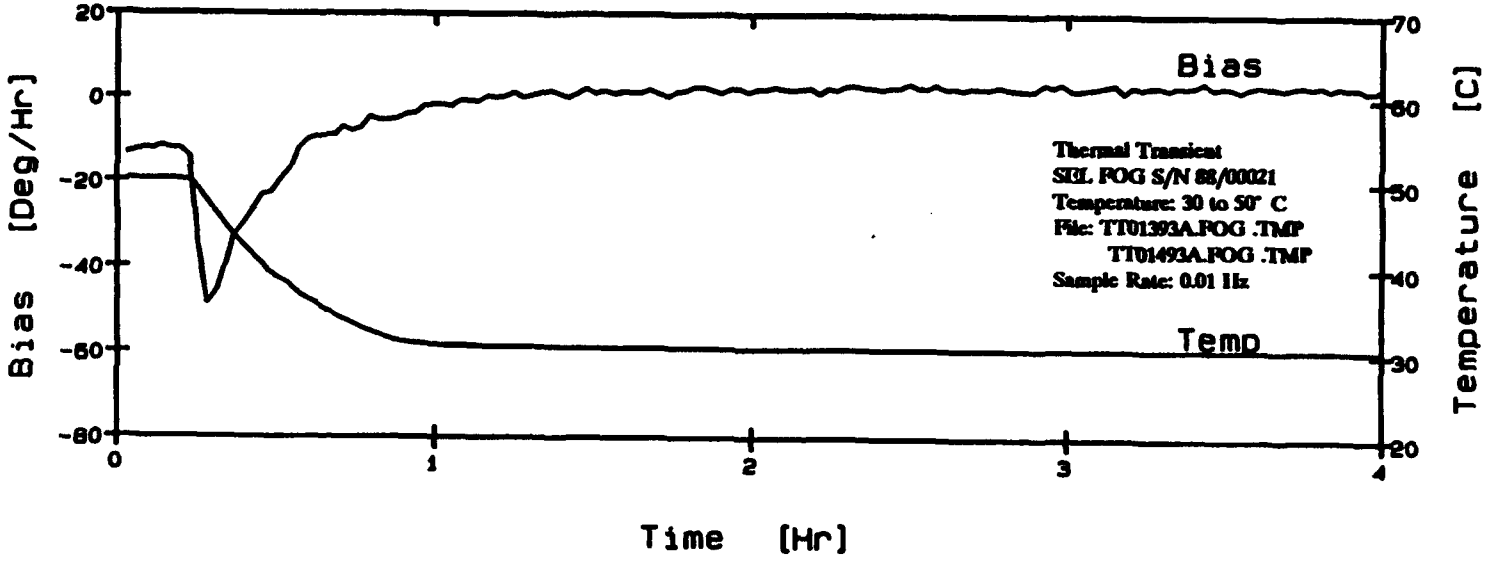

FIGURE 16(b): Thermal Transient 50-30°C

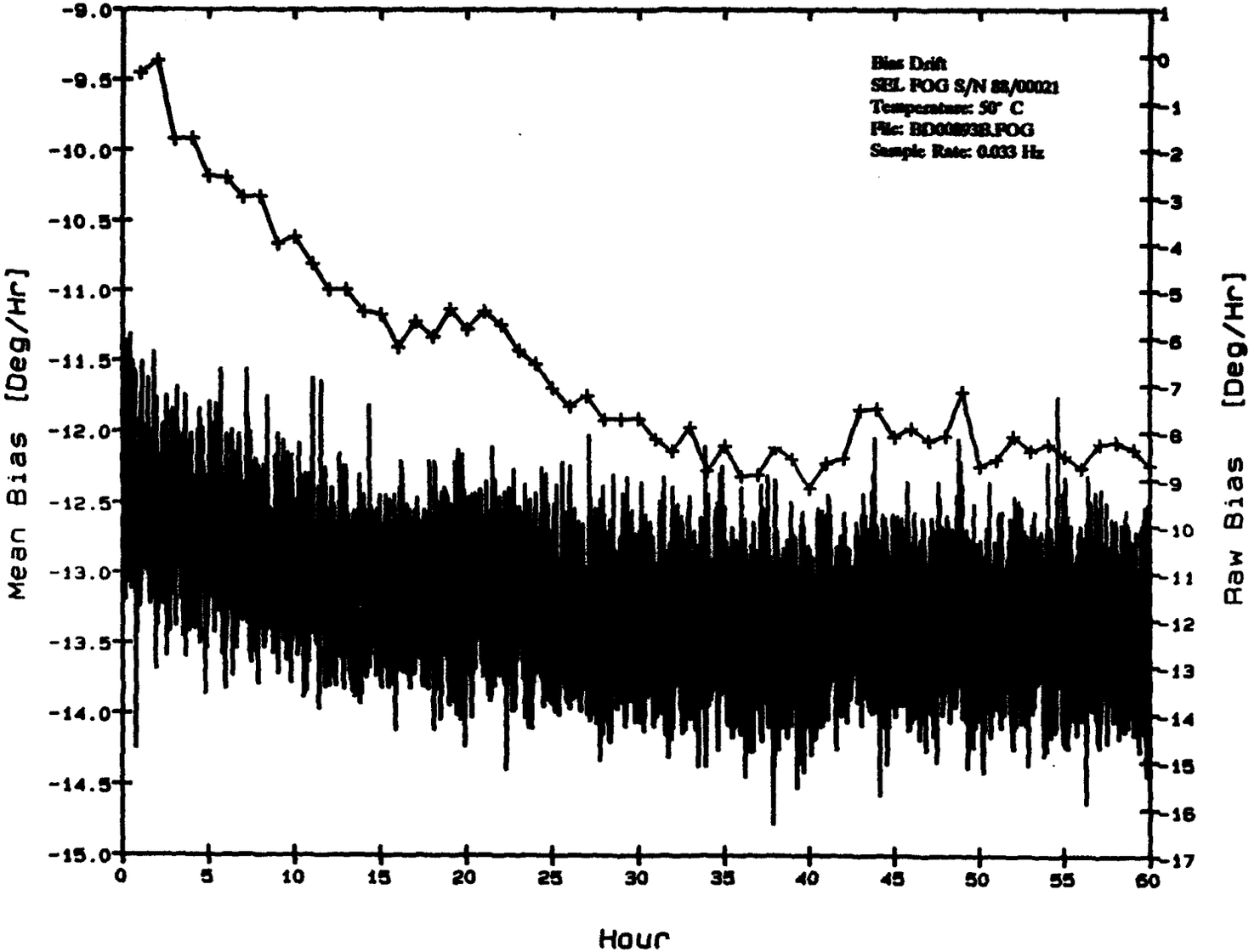

FIGURE 17: 60 Hour Bias Drift Test, 50°C

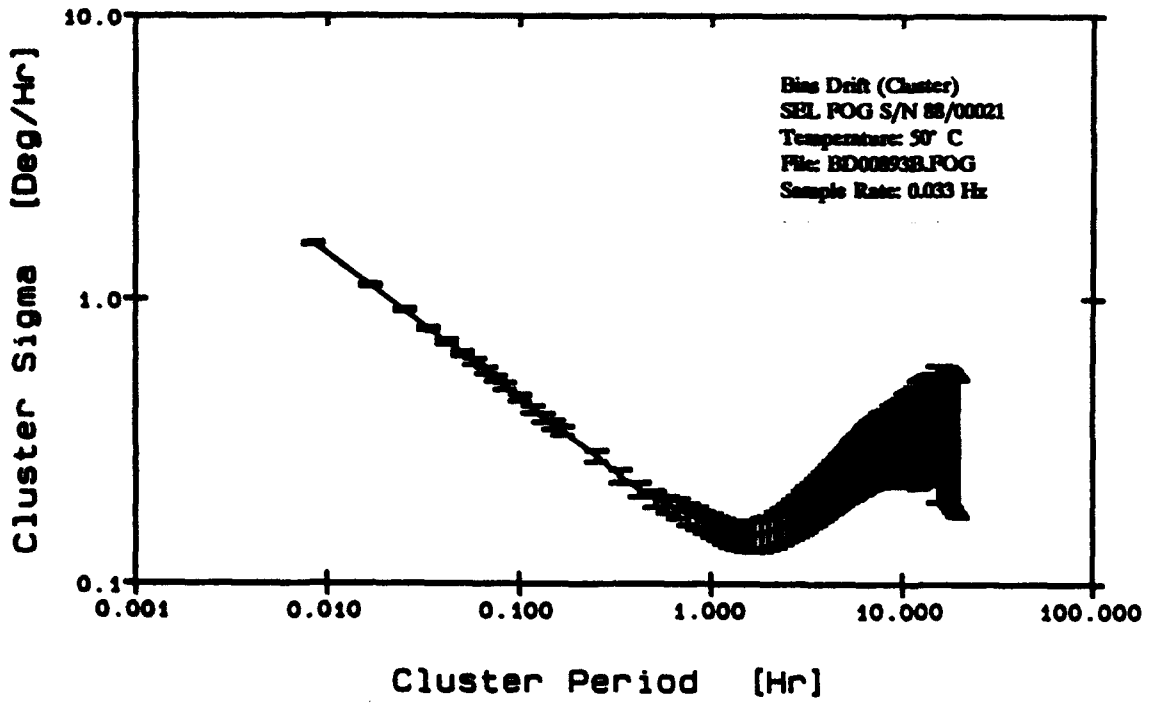

FIGURE 18: Rate Cluster Analysis at 50°C

5.3.4 Scale Factor

There are several types of gyro scale factor errors of interest to us. These include scale factor nonlinearity (often expressed as scale factor 'deviation'), scale factor repeatability (turn-on to turn-on and long-term), scale factor asymmetry (difference in scale factor in opposite directions of rotation) and scale factor stability (changes in scale factor under a constant rate input). In addition, of course, temperature sensitivity must be investigated.

Scale factor linearity (deviation) was determined over the entire operating rate range of the instrument ($\approx \pm$ 400 deg/sec). It should be noted that this instrument was designed specifically for the 10 to 100 deg/sec application range [2] and , although tests were conducted outside this range, they were considered to be for purposes of investigation ('enlightenment') only and are presented as such here. Figure 19 is a plot of the scale factor over the rate range of $\pm$ 0.1 to $\pm$ 400 deg/sec taken at a gyro operating temperature of 30°C.

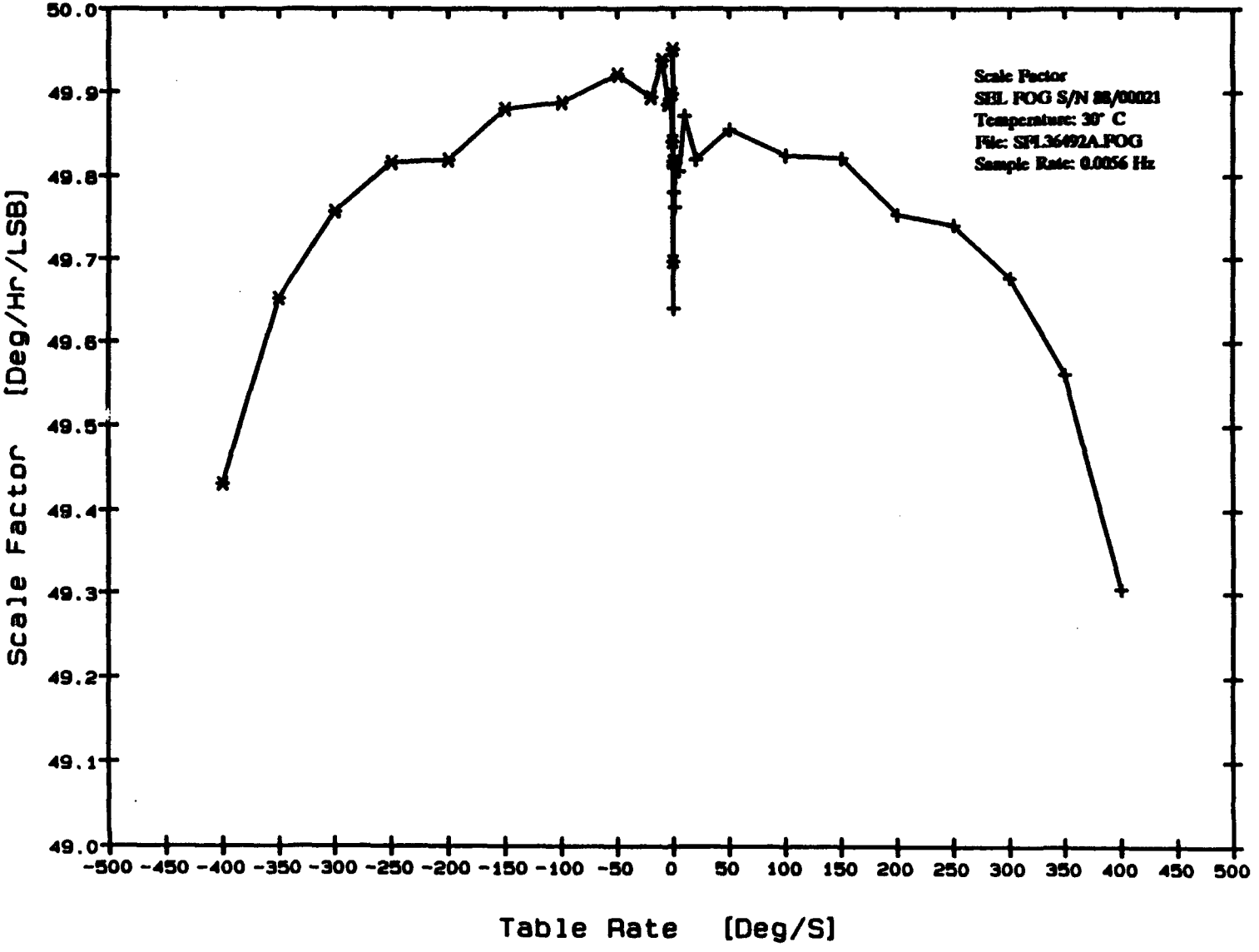

FIGURE 19: Scale Factor

The scale factor over the entire rate range varies from 49.95 deg/hr/LSB at -0.1 deg/sec to 49.31 deg/hr/LSB at +400 deg/sec or a total deviation of ≈13,000 ppm. In the range of most interest (10 to 100 deg/sec) the scale factor deviation drops to ≈ 1,000 ppm.

Figure 20 is an expanded view of the scale factor at low rates. The errors at these rates can be attributed to noise in the bias drift and light source instabilities. Thermal sensitivity is also more evident at low rates.

Scale factor asymmetry is demonstrated in Figure 21 where the negative rates (denoted by '*') from Figure 19 have been 'flipped over' for comparison purposes. There is a distinct bias offset between positive and negative rates of ≈ 1300ppm but, in the range of interest, 10-100 deg/sec, there is very little apparent asymmetry.

This can be verified by examination of Table 5 which contains the calculated scale factor over a ± 400 deg/sec rate range for temperatures of 30,40 and 50°C. Comparison of positive and negative rates shows asymmetry of, typically, less than 100 ppm which is well within the 'noise' level of the measurements.

Similarly from Table 5, scale factor repeatability is also available. Turn-on to turn-on scale factor repeatability is typically less than 1000 ppm in the range of 10-100 deg/sec. This is also illustrated in Figure 22 where the gyro is subjected to rate changes from 0 to 100 deg/sec. Samples are taken at 1KHz and the 'overshoot' at each rate change is actually due to the motion table; bandwidth of the Contraves motion table is approximately 10 Hz. Scale factor stability is demonstrated in Figure 23 where the gyro is subjected to a constant rate of 100 deg/sec for one hour. The rate stability of the DREO motion table has been shown to be ≈1ppm (peak-to-peak), therefore, variations in gyro output can be attributed to apparent scale factor variations (instability). The peak-to-peak scale factor stability is seen to be ≈1000ppm.

5.3.5 Scale Factor Temperature Sensitivity

Scale factor temperature sensitivity can be expected to be similar in nature to that of bias temperature sensitivity where increased temperature results in higher noise levels. The scale factor data from Table 5 is plotted in Figure 24 where two plots each at 30°C, 40°C and 50°C are shown. Note that the bias offset between positive and negative rates repeats for all curves and temperatures, scale factor asymmetry is negligible, and scale factor repeatability for the curves at 30 and 40°C is ≈1000ppm but a significant shift in scale factor occurs as temperature is increased to 50°C.

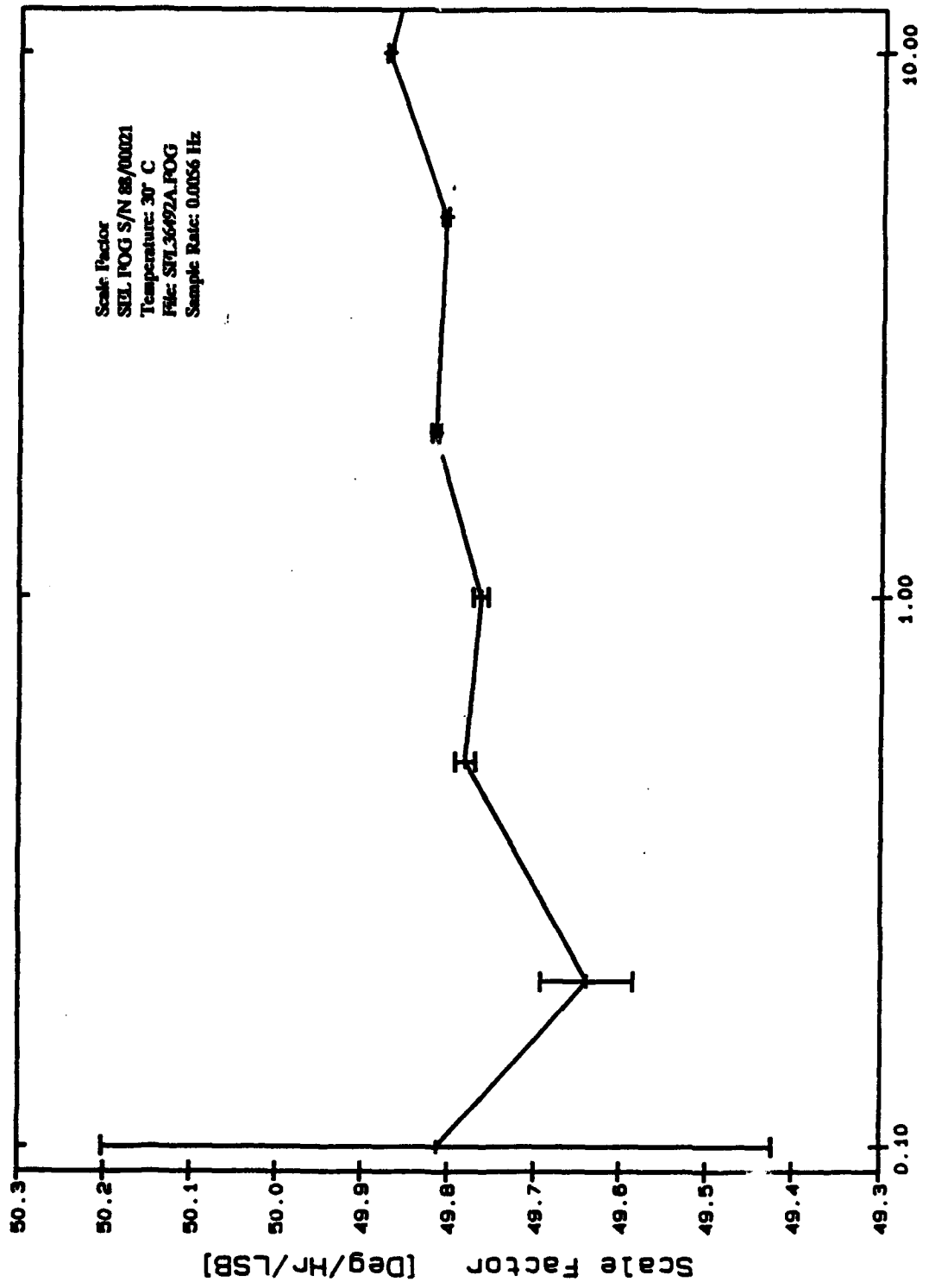

FIGURE 20: Scale Factor at Low Rate

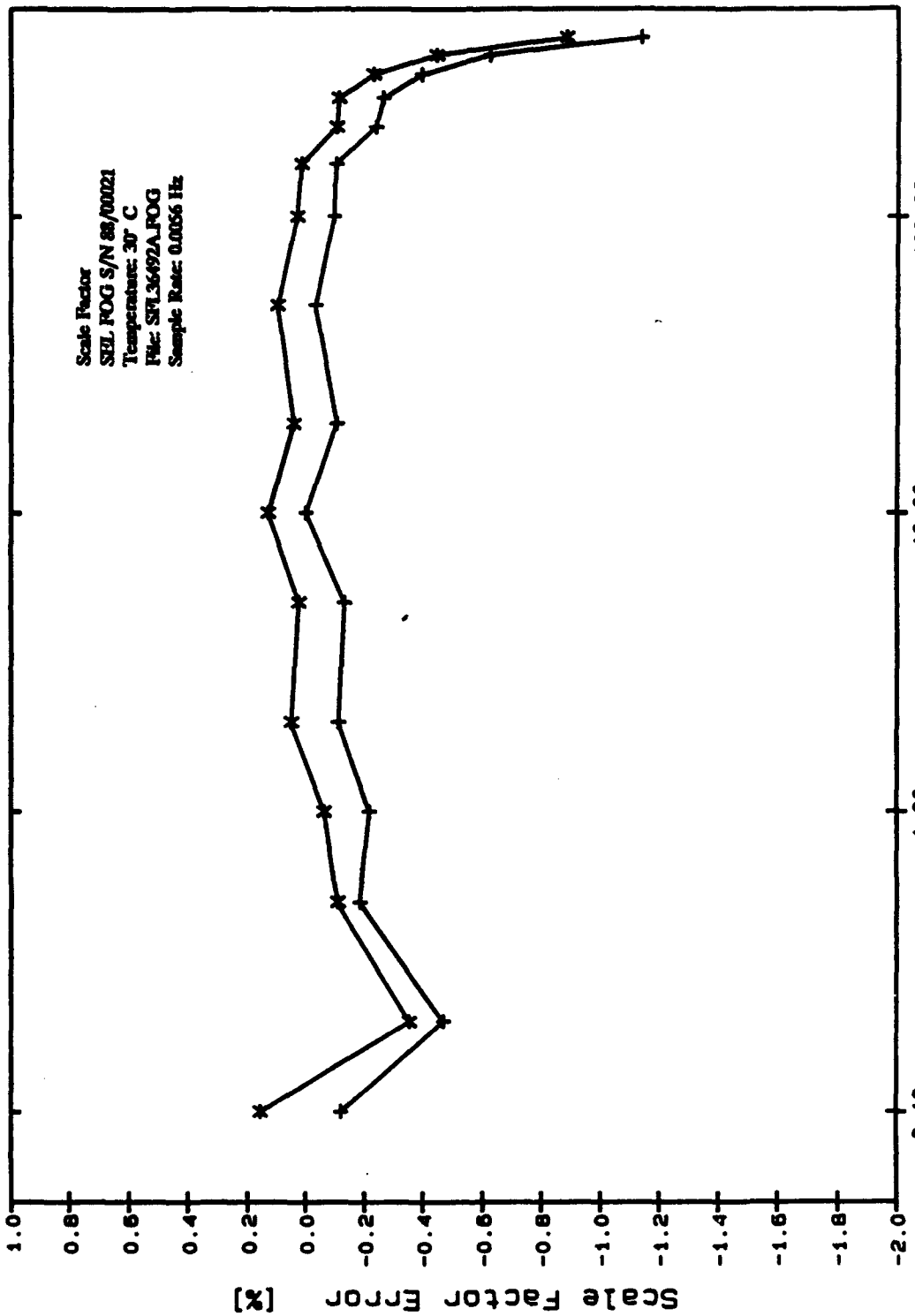

FIGURE 21: Scale Factor Asymmetry

	1 TBL Rate [Deg/S]	2 SFL36492A @ 30 C	3 SFL36592A @ 30 C	4 SFL00693A @ 40 C	5 SFL00793A @ 40 C	6 SFL01193A @ 50 C	7 SFL01293A @ 50 C
1	-400.00	49.430922	49.462803	49.418742	49.614490	52.953101	53.352898
2	-350.00	49.651733	49.675477	49.680057	49.832359	52.427357	52.766789
3	-300.00	49.758367	49.780288	49.842577	49.956635	52.176119	52.470691
4	-250.0	49.816287	49.830207	49.876670	50.008131	52.015309	52.276882
5	-200.0	49.819202	49.849747	49.944796	50.042848	51.889072	52.117239
6	-150.0	49.879378	49.887401	49.945137	50.06128	51.806291	52.027628
7	-100.0	49.887470	49.916960	50.009030	50.092938	51.749541	51.960762
8	-50.0	49.920514	49.914766	50.000104	50.106904	51.749470	51.959693
9	-20.0	49.893955	49.927532	50.019820	50.111146	51.736634	51.9433495
10	-10.0	49.937516	49.934322	50.019737	50.127693	51.765327	51.969492
11	-5.0	49.884877	49.925098	50.011530	50.099336	51.717109	51.932420
12	-2.0	49.897502	49.887995	49.987330	50.092811	51.725884	51.923776
13	-1.0	49.841200	49.892592	50.002014	50.86817	51.680180	51.912919
14	-0.5	49.817750	49.791980	49.975151	50.054504	51.675136	51.873348
15	-0.2	49.696986	49.794597	49.881186	50.054504	51.455769	51.773233
16	-0.1	49.950743	49.758808	50.019452	50.074416	51.761323	51.963048
17	0.1	49.812511	49.956288	49.945892	50.154643	51.977303	51.911347
18	0.2	49.639425	49.804242	49.939310	50.055269	51.523522	51.757230

TABLE 5: Scale Factor Test Data at 30, 40 and 50°C

	1 TBL Rate [Deg/S]	2 SFL36492A @ 30 C	3 SFL36592A @ 30 C	4 SFL00693A @ 40 C	5 SFL00793A @ 40 C	6 SFL01193A @ 50 C	7 SFL01293A A 50 C
19	0.5	49.781101	49.844927	49.927051	50.020842	51.592488	51.790513
20	1.0	49.763692	49.889550	49.996459	50.040032	51.641408	51.859300
21	2.0	49.816750	49.885610	49.966724	50.043023	51.661825	51.879590
22	5.0	49.805923	49.927771	50.025555	50.072870	51.668194	51.899089
23	10.0	49.871885	49.945587	50.016832	50.092651	51.708960	51.934712
24	20.0	49.820494	49.935625	50.037479	50.082392	51.686639	51.918849
25	50.0	49.855280	49.929642	49.99881	50.070804	51.697769	51.927843
26	100.0	49.824839	49.933189	50.025571	50.076385	51.705591	51.940135
27	150.0	49.821279	49.897203	49.960996	50.029775	51.744405	51.981593
28	200.0	49.754060	49.877043	49.958266	50.014355	51.829116	52.098794
29	250.0	49.741571	49.847121	49.892817	49.962614	51.955308	52.241722
30	300.0	49.676825	49.817886	49.852269	49.924190	52.103374	52.435779
31	350.0	49.561739	49.705795	49.682008	49.781756	52.351494	52.727707
32	400.0	49.305407	49.521547	49.442581	49.556557	52.855948	53.307073
	mean	49.779	49.842	49.916	50.013	51.875	52.120
	Std dev	0.141	0.116	0.154	0.137	0.346	0.403
	ptop	0.645	0.493	0.619	0.598	1.497	1.596

TABLE 5: (Continued)

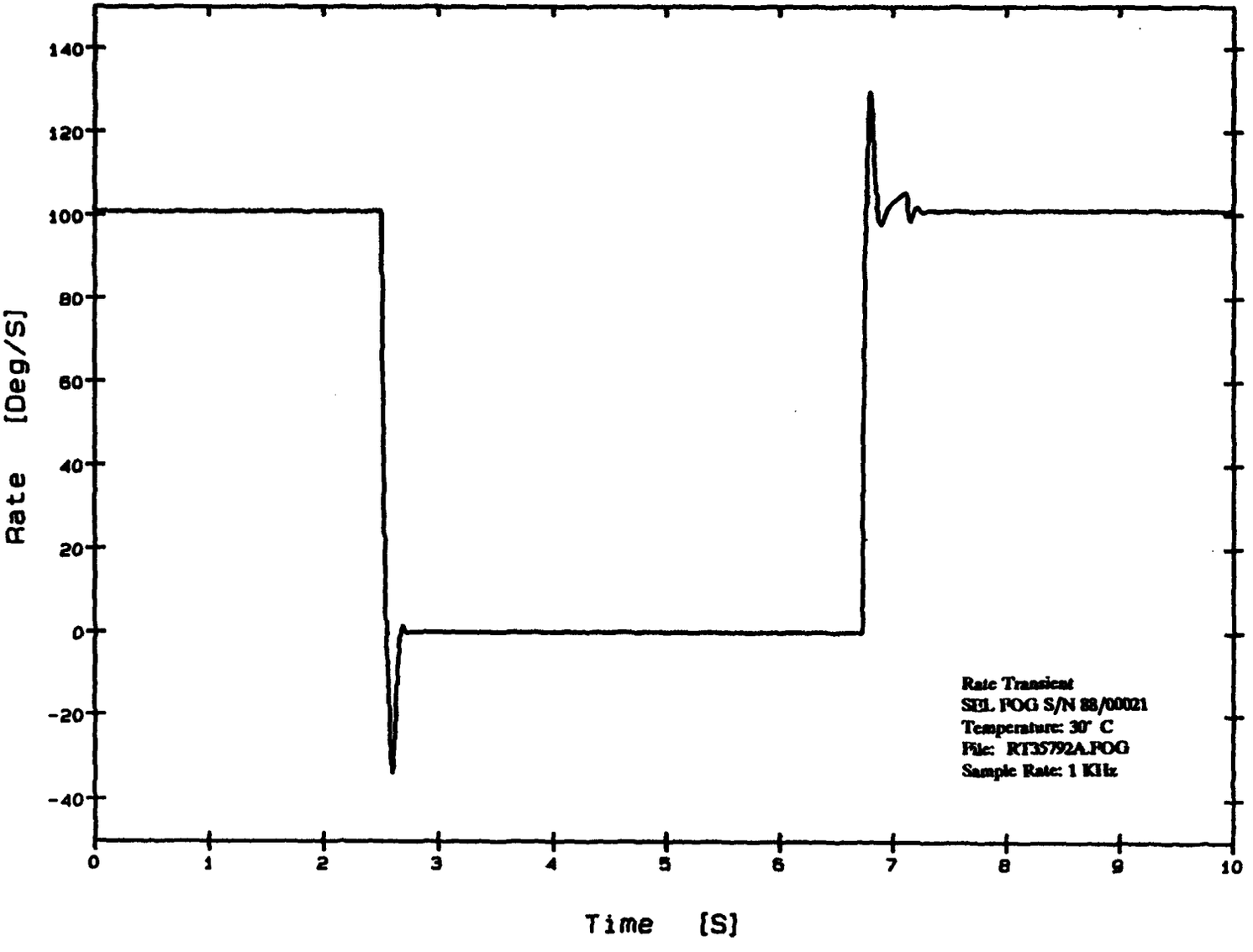

FIGURE 22: Rate Transients

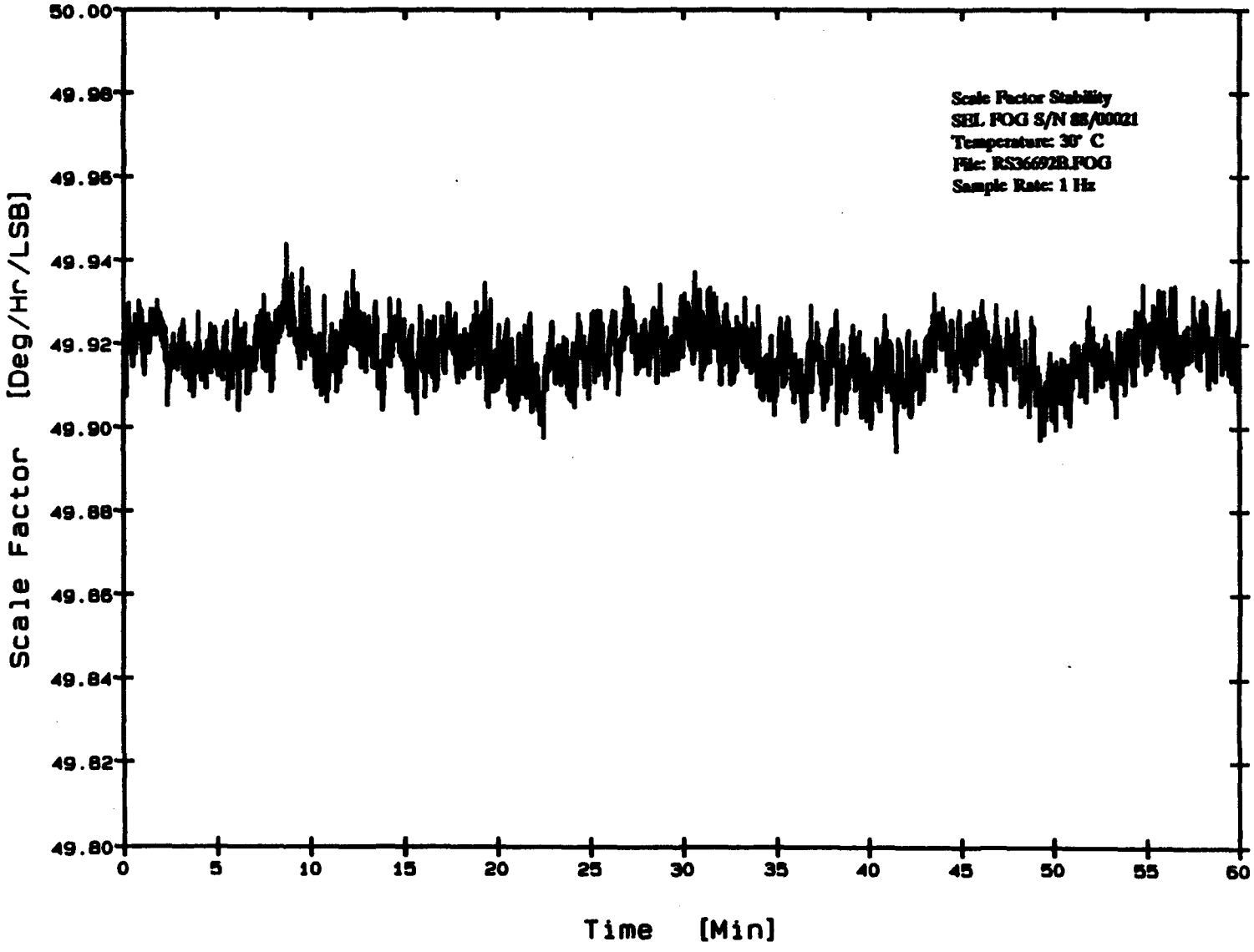

FIGURE 23: Scale Factor Stability

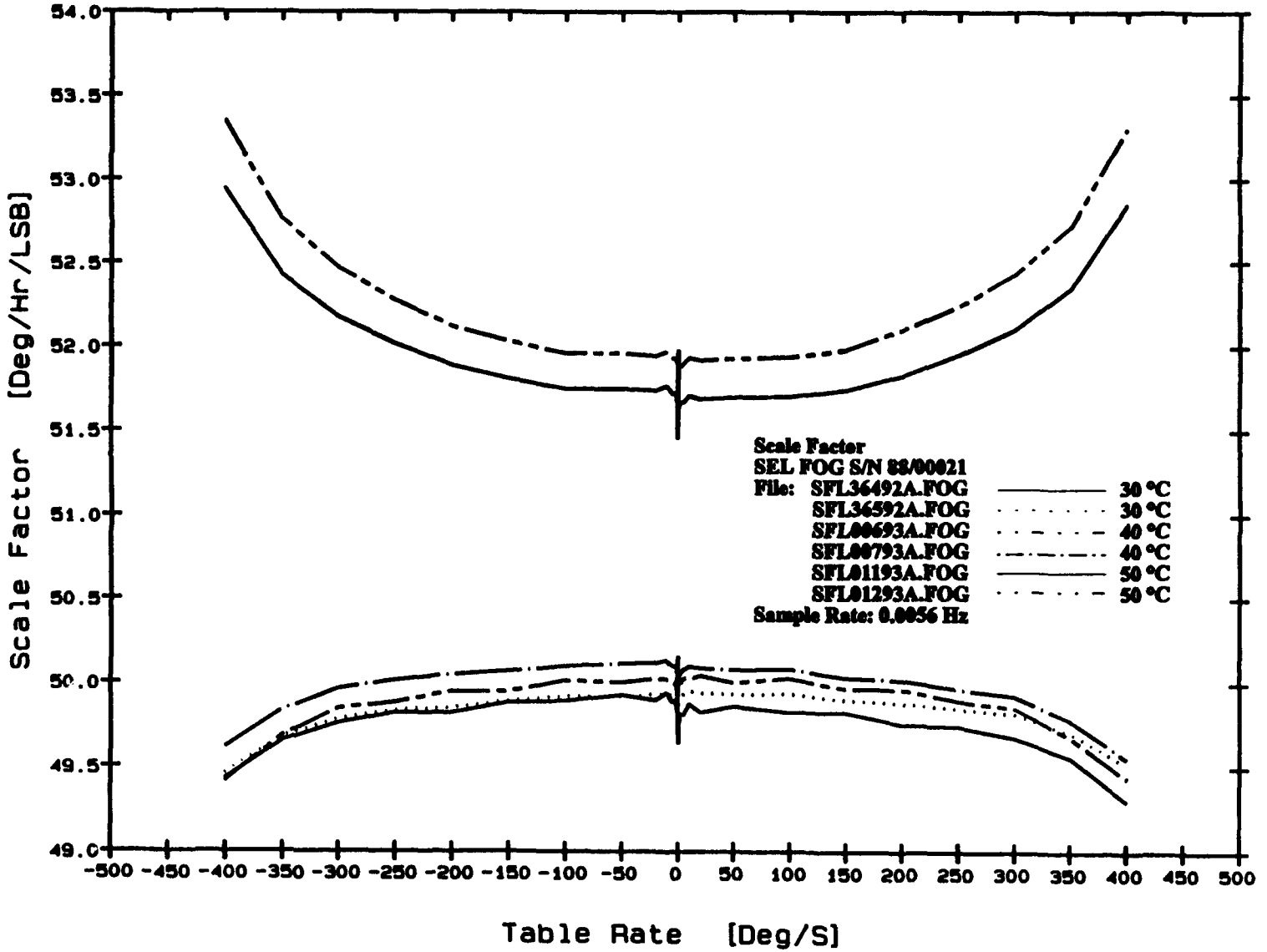

FIGURE 24: Scale Factor Deviation at 30,40 and 50°C

At 50°C, the scale factor apparently shifts with respect to 30°C by >30,000ppm in the 10-100 deg sec range and the repeatability degrades to ≈3,000ppm. Note, also, the change in shape of the curves, particularly at increased angular rates. The specific cause of this effect is unknown but from data taken subsequent to this set of tests at 50°C, it appears that the gyroscope underwent a permanent shift in bias and scale factor and never recovered. Since this data set marked the final set of tests to be performed on the instrument, it was decided to complete the test program with the final test; thermal transient effects on scale factor and evaluate the data.

Thermal transient tests, similar to those used to investigate bias sensitivity are illustrated in Figure 25. In Fig 25(a), a thermal transient from 30°C to 50°C at ≈2°C/min results in a scale factor shift of ≈5700ppm, a far cry from the apparent 30,000ppm shift seen in Figure 24. But one may note in Figure 25(a), that the scale factor determined at 30°C is 52.28 deg/hr/LSB whereas in previous tests we have shown the scale factor was ≈49.80 deg/hr/LSB at 30°C; an apparent scale factor shift. This is confirmed in Figure 25(b) where the temperature is reduced from 50°C to 30°C and the scale factor returns to (and remains at) ≈52.3 deg/hr/LSB. This shift does not appear to have changed the performance of the gyro and the exact cause remains unexplained.

FIGURE 25(a): Thermal Transient, 30-50°C

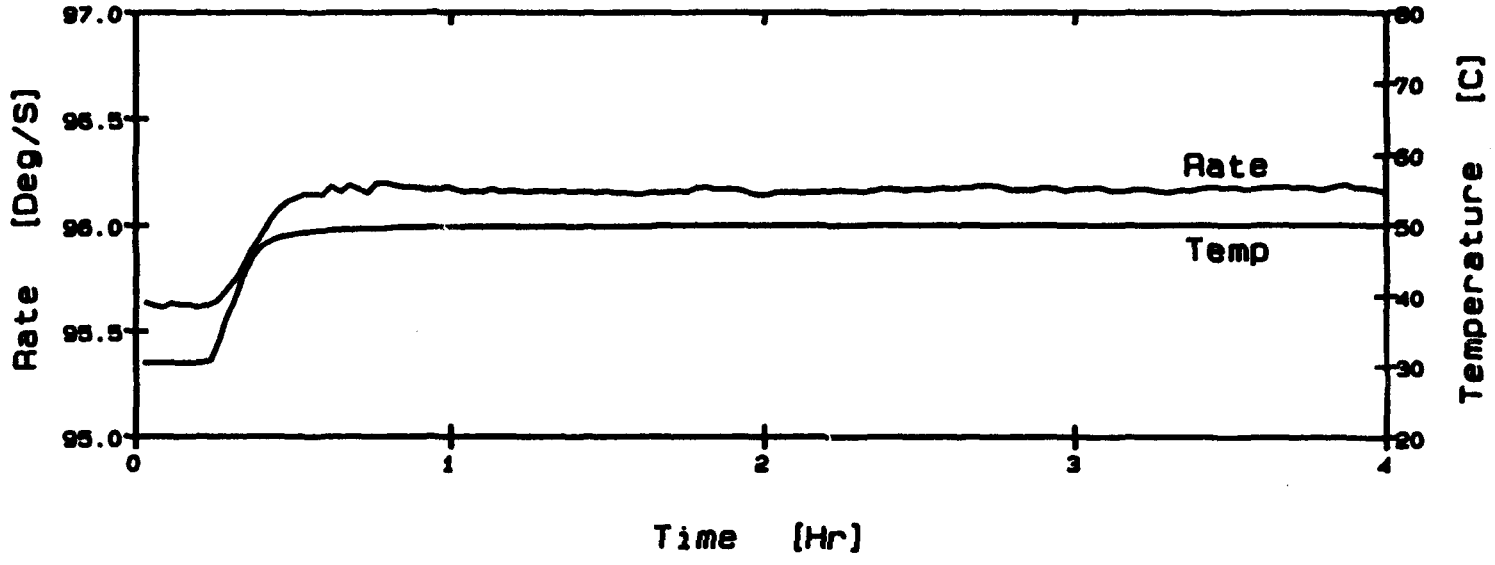

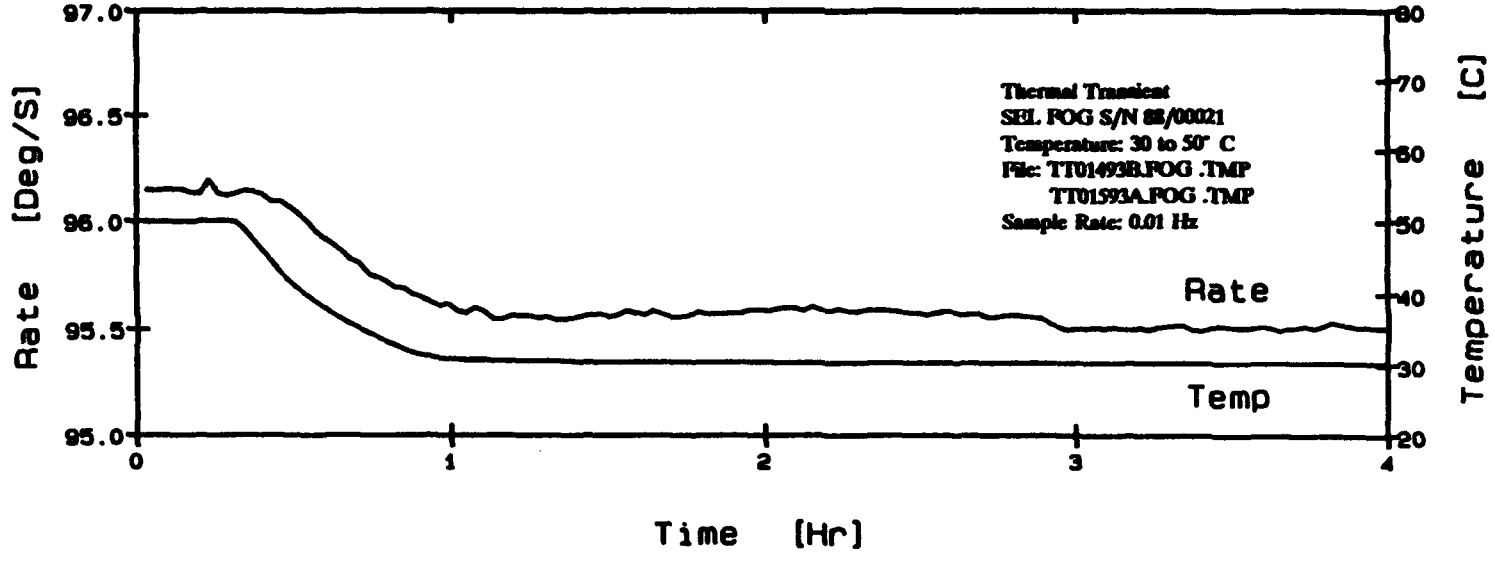

FIGURE 25(b): Thermal Transient, 50-30°C

6.0 CONCLUSIONS

6.1 Data Summary

Table 6 and Figures 26, 27 and 28 encompass the test results on the SEL FOG, S/N 88/0021, as determined by tests at SEL and provided to DREO with the gyroscope.

Nominal scale factor (temperature unknown) is stated to be 49.99 deg/hr/LSB and our results indicate a temperature-sensitive bias varying from 49.78 deg/hr/LSB at 30°C to 52.12 deg/hr/LSB at 50°C (before the 'shift', previously described).

Scale factor deviation over the rate range of $\pm$ 400 deg/sec is quoted at <5000ppm, but, upon inspection of Figure 26, the actual data plots indicate a peak-to-peak deviation of close to 9000ppm. In our case, scale factor deviation was 13,000ppm but, in both sets of data, deviation over the 10-100 deg/sec range was substantially better.

Temperature sensitivity of both bias and scale factor is very significant in this instrument with bias varying $\pm$ 20 deg/hr over a temperature range of 25 to 50°C as shown in Figure 27. We have demonstrated bias changes of ≈15 deg/hr over a temperature change of 30 to 50°C. In addition, the rate at which the temperature changes has been shown to seriously affect the bias drift, apparently defeating the thermal compensation scheme employed in the gyro.

Scale factor temperature sensitivity as demonstrated in Figure 28 shows a scale factor change of 0.3 deg/hr/LSB or ≈ 5900ppm over a 25°C to 50°C temperature change. Similarly, we found a 5700ppm change.

In total, approximately 480 hours of test data was accumulated from the gyro.

1. **PART LIST**

Sensor:	PO1DE	88/00021
Signal Processing Board:	PE1DE	88/00021
Power Supply Board:	SVFA	88/00021
Board housing and cable set		

2. **ELECTRICAL INTERFACE**

Power:

Operating Voltage:	+28 V DC (+9...+35 V DC)
Input Current:	1 A (max)
Signal Output:	16 bit parallel, open collector, active low, two's complement
Monitor:	serial, RS-232C
Self Test:	NOGO line (active low) set in case of poor functioning
Signal:	Digital, proportional to rotation rate, positive clockwise rotation looking down on sensor
Repetition rate:	971 Hz

3. **Performance:**

Measuring Range:	$\pm$ 400 deg/s
Scale Factor:	49.99 deg/h / LSB
Scale Factor Error:	$<0.5\%$ (1σ)
Bandwidth:	500 Hz
Resolution (Noise):	<10 deg/h/$\sqrt{\text{Hz}}$
Bias Uncertainty:	<10 deg/h (1σ)
Turn On Time:	<1s

4. **Environment:**

Temperature Range:	
Operation:	-40...+71°C
Storage	-54...+71°C
Humidity:	95% relative
Vibration:	20 Hz...2kHz, 10g, sine (sensor)
Shock:	100g, 11ms, sine-halfwave (sensor)

TABLE 6: SELF Fibre Optic Gyroscope Specifications and Performance

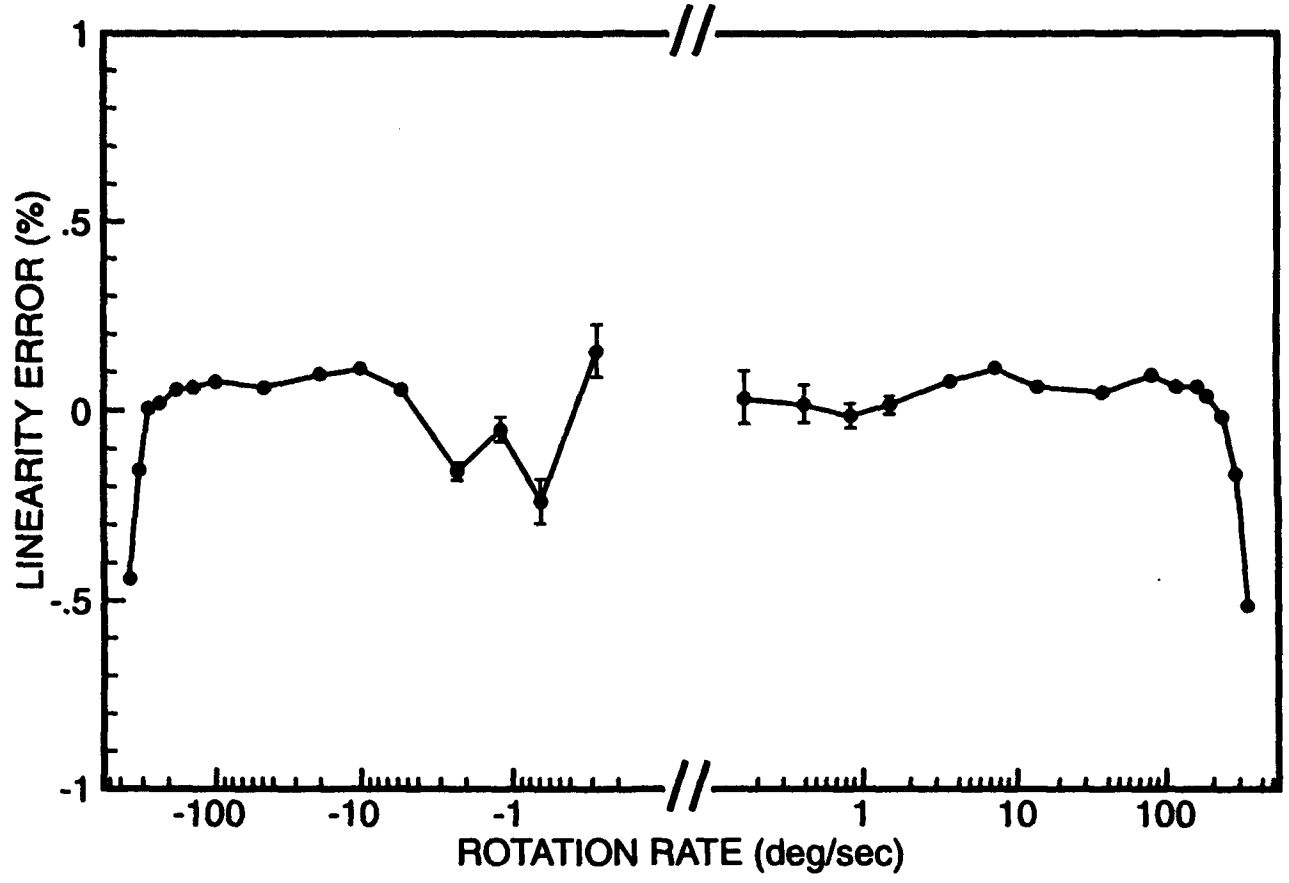

FIGURE 26: Scale Factor Deviation (SEL Test Data)

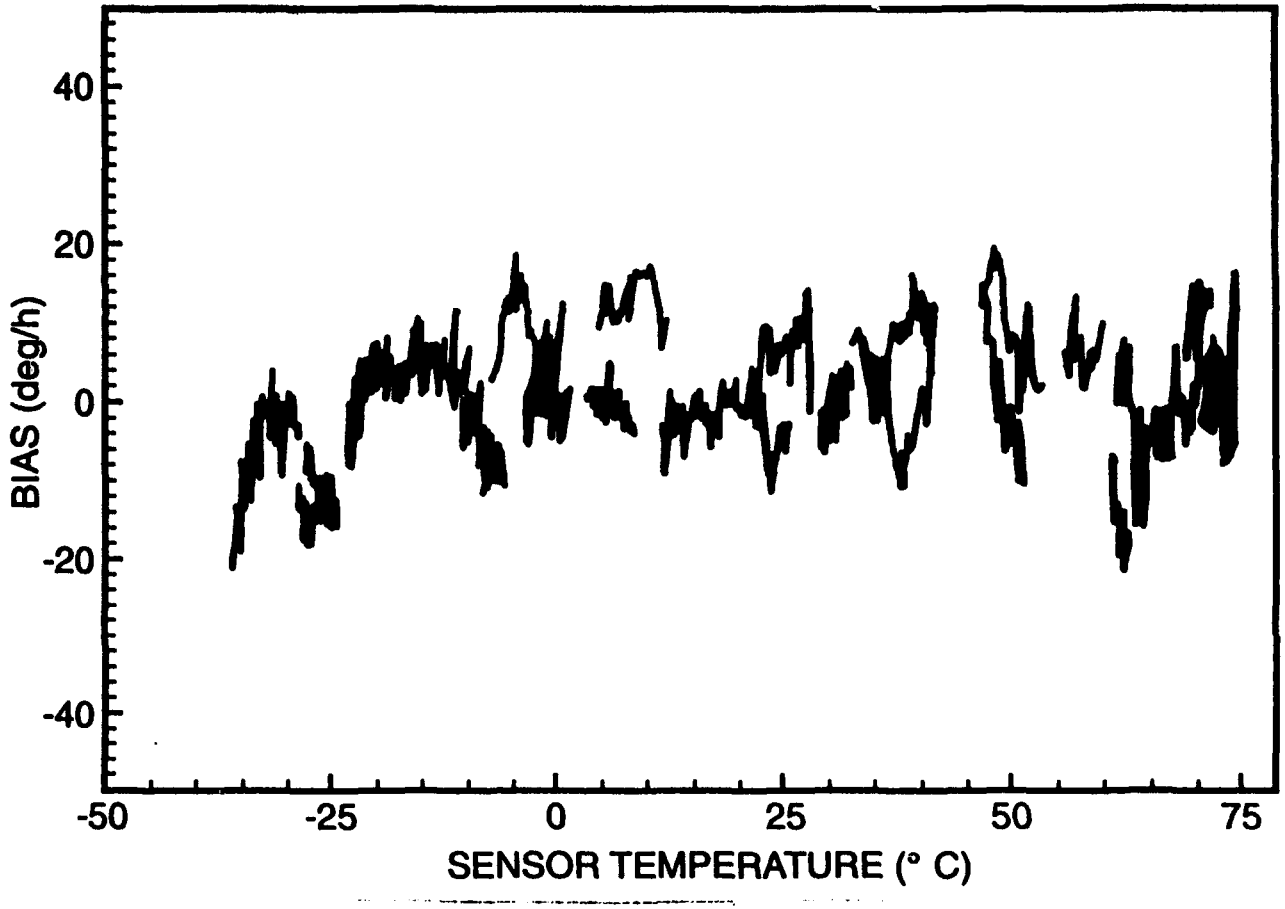

FIGURE 27: Bias Temperature Sensitivity (SEL Test Data)

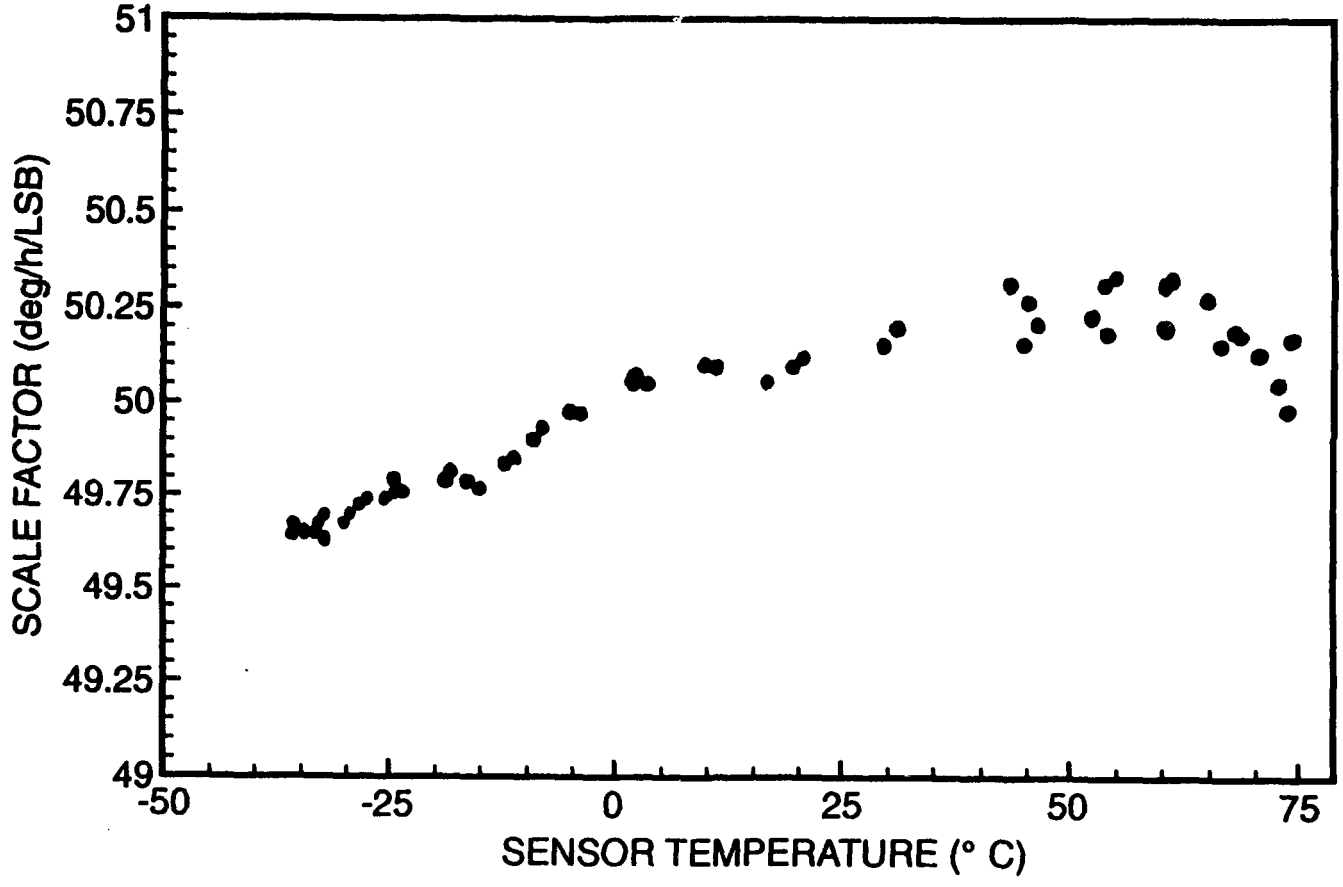

FIGURE 28: Scale Factor Temperature Sensitivity (SEL Test Data)

6.2 General Comments

The SEL FOG, one of the first commercially-available instruments of its kind, appears to be a functional, reliable gyroscope over the dynamic range of $\pm$ 400 deg/sec.

The sources of errors in bias and scale factor in a fibre optic gyroscope are well documented [8] [11] [12] and will not be analyzed here but, in many cases, the primary cause is temperature; temperature gradients which result in thermal nonreciprocity and cause bias instability or temperature changes which cause scale factor errors by changing the geometric size of the fibre coil. Aging effects are also significant whereby source wavelength or power are reduced resulting in increased random noise and scale factor error. The results of our tests, as presented here, confirm these temperature-related effects. The dramatic shift in bias and scale factor at higher temperature may be an aging-related effect.

7.0 REFERENCES

1. J.S. Sinkiewicz, D. Cardarelli, 'Fibre Optic Gyroscope Technology Development; Its Evaluation and a Present Day Survey,' Inertial Engineering Inc., Final Report Contract No. 04ST.W7714-1-9542, April 1992

2. W. Auch, M. Oswald, 'Development of a Fibre-Optic Rate Gyro for Military Applications,' Proceeding of Sixth European Fibre Optic Communications and Local Area Networks Exposition (EFOC/LAN 88), 29 June - 1 July 1988.

3. 'SEL Fibre Gyro PM1DE,' SEL gyroscope specification document delivered with gyroscope S/N 88/00021.

4. J.P. Thomas Goguen, 'DREO Navlab SEL, Fibre Optic Gyro Data Collection System,' CARO Engineering Inc., Report, Contract No. W7714-2-9640/01-ST, February 1993.

5. J.P. Thomas Goguen, 'Navlab Data Collection Software User's Manual', CARO Engineering Inc., Report, Contract No. W7714-8-5668, July 1988.

6. M.F. Vinnins, 'The DREO Inertial Navigation Laboratory: Development and Test Capabilities,' DREO Report No. 895, June 1984.

7. M.M. Tehrani, 'Ring Laser Gyro Data Analysis with Cluster Sampling Technique,' Proceedings of Fibre-Optic and Laser Sensors, SPIE Vol 412, 1983.

8. R.Y. Lui, T.F. El-Wailly, R.C. Dankwort, 'Test Results of Honeywell's First-Generation, High Performance Interferometric Fibre-Optic Gyroscope,' Fibre Optic Gyros: 15th Anniversary Conference, SPIE Vol. 1585, 1991.

9. 'IEEE Standard Inertial Sensor Terminology', IEEE Std 528-1984, IEEE Inc., New York, January 1984.

10. J.P. Thomas Goguen, 'DREO Navlab SEL Fibre Optic Gyroscope Rate Cluster Analysis,' CARO Engineering Inc. Report, Contract No. W7714-2-9640/01-ST, January 1993.

11. H.C. Lefevre, H.J. Arditty, 'Fibre-Optic Gyroscope,' Selected Paper on Fibre-Optic Gyroscopes, SPIE Milestone Series, Vol MS8, 1989.

12. R. Ruffin, C.C. Sung, R. Morgan, 'Analysis of Temperature and Stress Effects in Fibre Optic Gyroscopes,' Fibre Optic Gyros: 15th Anniverary Conferences, SPIE Vol 1585, 1991.

UNCLASSIFIED

SECURITY CLASSIFICATION OF FORM

(highest classification of Title, Abstract, Keywords)

DOCUMENT CONTROL DATA

(Security classification of title, body of abstract and indexing annotation must be entered when the overall document is classified)

1. ORIGINATOR (the name and address of the organization preparing the document. Organizations for whom the document was prepared, e.g. Establishment sponsoring a contractor's report, or tasking agency, are entered in section 8.)

Defence Research Establishment Ottawa
Electronics Division/Communications & Navigation Section
Ottawa, Ontario, CANADA K1A OK2

2. SECURITY CLASSIFICATION (overall security classification of the document including special warning terms if applicable)

UNCLASSIFIED

3. TITLE (the complete document title as indicated on the title page. Its classification should be indicated by the appropriate abbreviation (S,C or U) in parentheses after the title.)

LABORATORY EVALUATION OF THE STANDARD ELECTRIK LORENZ (SEL) FIBRE-OPTIC RATE GYROSCOPE (U)

4. AUTHORS (Last name, first name, middle initial)

VINNINS, MICHAEL F., GALLOP, LLOYD D.

5. DATE OF PUBLICATION (month and year of publication of document)

November 1993

6a. NO. OF PAGES (total containing information. Include Annexes, Appendices, etc.)

51

6b. NO. OF REFS (total cited in document)

12

7. DESCRIPTIVE NOTES (the category of the document, e.g. technical report, technical note or memorandum. If appropriate, enter the type of report, e.g. interim, progress, summary, annual or final. Give the inclusive dates when a specific reporting period is covered.

DREO Report

8. SPONSORING ACTIVITY (the name of the department project office or laboratory sponsoring the research and development. Include the address.

DEFENCE RESEARCH ESTABLISHMENT OTTAWA, ELECTRONICS DIVISION
COMMUNICATIONS AND NAVIGATION SECTION, OTTAWA, ONTARIO K1A OK2

9a. PROJECT OR GRANT NO. (if appropriate, the applicable research and development project or grant number under which the document was written. Please specify whether project or grant)

041LJ

9b. CONTRACT NO. (if appropriate, the applicable number under which the document was written)

10a. ORIGINATOR'S DOCUMENT NUMBER (the official document number by which the document is identified by the originating activity. This number must be unique to this document.)

DREO REPORT 1210

10b. OTHER DOCUMENT NOS. (Any other numbers which may be assigned this document either by the originator or by the sponsor)

11. DOCUMENT AVAILABILITY (any limitations on further dissemination of the document, other than those imposed by security classification)

(X) Unlimited distribution
( ) Distribution limited to defence departments and defence contractors; further distribution only as approved
( ) Distribution limited to defence departments and Canadian defence contractors; further distribution only as approved
( ) Distribution limited to government departments and agencies; further distribution only as approved
( ) Distribution limited to defence departments; further distribution only as approved
( ) Other (please specify):

12. DOCUMENT ANNOUNCEMENT (any limitation to the bibliographic announcement of this document. This will normally correspond to the Document Availability (11). however, where further distribution (beyond the audience specified in 11) is possible, a wider announcement audience may be selected.)

Unlimited Announcement

UNCLASSIFIED

SECURITY CLASSIFICATION OF FORM

RA.W (17 Dec 90)

13. **ABSTRACT** (a brief and factual summary of the document. It may also appear elsewhere in the body of the document itself. It is highly desirable that the abstract of classified documents be unclassified. Each paragraph of the abstract shall begin with an indication of the security classification of the information in the paragraph (unless the document itself is unclassified) represented as (S), (C), or (U). It is not necessary to include here abstracts in both official languages unless the text is bilingual).

A fibre-optic rate-sensing gyroscope (FOG) manufactured by Standard Elektrick Lorenz (SEL) was loaned to DREO for evaluation. The SEL FOG, model PM1DE, was designed for a drift rate of 10 to 100 deg/hr and consists of two units; a fibre-optic sensor and a support electronics unit. Laboratory tests were carried out in the DREO Inertial Navigation Laboratory and consisted of bias drift and scale factor over ± 400 deg/sec as well as temperature sensitivity. Performance data obtained by DREO agreed closely with predicted performance although bias drift demonstrated wide deviations under thermal rate-transients. A permanent shift in bias drift and scale factor also occured after extended testing at 50°C. A bias drift of 5.38 deg/hr ± 0.68 deg/hr was achieved at 30°C and scale factor deviation was ≈ 13,000 ppm over a rate range of 400 deg/sec. This instrument would be suitable for a low-performance Attitude and Heading Reference System (AHRS) application.

14. **KEYWORDS, DESCRIPTORS or IDENTIFIERS** (technically meaningful terms or short phrases that characterize a document and could be helpful in cataloguing the document. They should be selected so that no security classification is required. Identifiers, such as equipment model designation, trade name, military project code name, geographic location may also be included. If possible keywords should be selected from a published thesaurus, e.g. Thesaurus of Engineering and Scientific Terms (TEST) and that thesaurus-identified. If it is not possible to select indexing terms which are Unclassified, the classification of each should be indicated as with the title.)

fibre-optic gyroscope
FOG
rate sensor